

FEYNMAN: KNOWLEDGE-INFUSED DIAGRAMMING AGENT FOR SCALING VISUAL REASONING DATA

Anonymous authors

Paper under double-blind review

ABSTRACT

Visual reasoning is an essential ability of state-of-the-art multi-modal AI systems. Improving these systems requires high-quality vision-language data at scale. Despite the abundance of internet image and text data, knowledge-rich and well-aligned image-text pairs are rare. In this paper, we present a scalable data generation pipeline built with our diagramming agent, FEYNMAN. To create diagrams, FEYNMAN first enumerates domain-specific knowledge components (“ideas”) and performs code planning based on the ideas. Given the plan, FEYNMAN translates ideas into simple declarative programs and iterates to receive feedback and visually refine diagrams. Finally, the declarative programs are rendered by the PENROSE diagramming system. The optimization-based rendering of PENROSE preserves the visual semantics while injecting fresh randomness into the layout, thereby producing diagrams with visual consistency and diversity. As a result, FEYNMAN can author diagrams along with grounded captions with very little cost and time. Using FEYNMAN, we synthesized a dataset with more than 100k well-aligned diagram-caption pairs. We also curate a visual-language benchmark, DIAGRAMMA, from freshly generated data. DIAGRAMMA evaluates the visual reasoning capabilities of vision-language models. We plan to release the dataset, benchmark, and the full agent pipeline as an open-source project.

1 INTRODUCTION

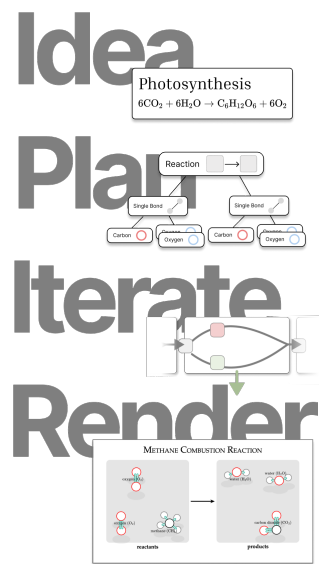


Fig. 1: The FEYNMAN Agent

A diagram is worth ten thousand words. Humans represent knowledge visually and solve complex problems efficiently using diagrams (Tversky, 2017; Larkin & Simon, 1987). However, the current generation of multi-modal large-language models (MLLMs) such as GPT-4V (Yang et al., 2023), Gemini (Team et al., 2023) and Llama 3 (Dubey et al., 2024b) still struggle to understand, use, and generate simple visual objects that often show up in diagrams, despite tremendous progress on general multi-modal benchmarks (Yue et al., 2024). Prior work have shown MLLMs to fail rudimentary vision tests (Rahmanzadehgervi et al., 2024), perceive graph structures poorly (Li et al., 2024d), and lack compositional understanding of visual attributes, relations, and ordering (Yuksekgonul et al., 2022). The important work (Zhang et al., 2024a) specifically demonstrated their weaknesses on reasoning with abstract mathematical diagrams.

Currently, training large models relies heavily on enormous amount of data for both pre- and post-training to make progress on any capabilities (Dubey et al., 2024a; Li et al., 2024c; Tong et al., 2024), including diagram understanding (McKinzie et al., 2024). To augment training data, one general strategy is to synthesize data using state-of-the-art large-language models. Unfortunately, synthesizing

vision-language data is challenging. Prevalent approaches of synthesizing vision-language data focus on the language side, such as augmenting instruction-following data from image captions (Li et al., 2022; Liu et al., 2024b; Wang et al., 2022). To synthesize images, the two main paradigms are diffusion models (Rombach et al., 2022) and graphics program synthesizers (Belouadi et al.,

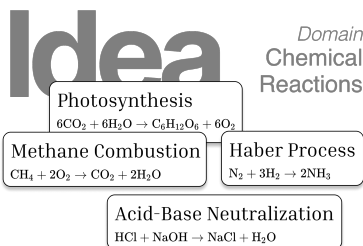


Figure 2(a): **Idea step**: In the first step, FEYNMAN enumerates the knowledge given a specific domain.

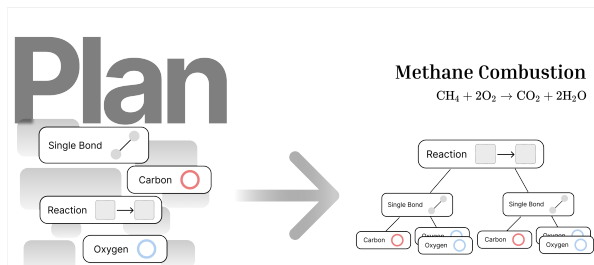


Figure 2(b): **Plan step**: Per idea, FEYNMAN then devises extract relevant elements such as chemical bonds and formulates a plan to translate them into Substance code.

2024b;c; Wu et al., 2023). The former generate raster images while the latter synthesize textual programs that produce vector graphics. Regardless of the output format, both approaches struggle to produce good diagrams consistently. Given the demand for high-quality synthetic diagrams and the limitations of current approaches, we ask the following research question:

Can we generate synthetic diagram-language pairs at scale?

When generating conceptual diagrams, models are tasked to perform both *knowledge elicitation* and *visual production*. When prompted to produce a diagram representing some high-level concepts, the model needs to elicit the relevant concepts (abstract knowledge, e.g., H_2O has 2 hydrogen and 1 oxygen atoms), map them to visual components (visual knowledge, e.g., use ball-and-stick model to represent molecules), and organize these components in an image (visual production). However, state-of-the-art diffusion and language models struggle because they are asked to perform these steps all at once. For instance, diffusion models can produce visually pleasing images but may ignore important concepts in the diagram; language models may include the right concepts in the image but the diagram layout can be poor and illegible. In this paper, we recognize this challenge of diagram generation, and ask:

Can we decouple knowledge elicitation and visual production in diagram synthesis?

To address our questions, we elicit domain knowledge from LLMs and iteratively produce high-quality diagrams using a knowledge-aware diagram interface. We propose FEYNMAN, an LLM agent that scales up diagram synthesis by decoupling knowledge elicitation and visual production. FEYNMAN leverages the knowledge advantage of modern LLMs by isolating knowledge elicitation as its first step in diagram synthesis. Instead of directly producing SVG source code or a raster image, FEYNMAN produces knowledge components (“ideas”), which are then translated to their visual representations. To ensure high-quality visual production, FEYNMAN utilizes the PENROSE language, which explicitly codifies the mapping from domain-specific concepts to their visual representations (Ye et al., 2020). The resulting diagram synthesis pipeline preserves the semantics of the diagrams, and we further utilize them to generate a diverse question-answer set tailored to the generated content. Overall, our contributions include:

1. We created a diagramming agent, FEYNMAN, to author knowledge-infused diagrams and achieves remarkable yield rate in generating textbook-level diagram examples. Powered by PENROSE, FEYNMAN generates diagrams with diverse visual content.
2. With FEYNMAN, we generated 10693 knowledge-infused programs, leading to the creation of 106930 well-aligned diagram-caption pairs. This was accomplished within 1,550 million input and output tokens at a cost of under \$400 with GPT-4o-mini.
3. We release a new benchmark DIAGRAMMA made of entirely fresh examples authored by FEYNMAN. We conducted a thorough quantitative evaluation of 17 MLLMs in Table 2
4. Via comprehensive ablations and analysis, we provide insights into how to build multi-modal AI agents that can work in the intersection of knowledge, visual design, and code generation. We analyze the economic aspects of synthesizing large-scale scientific diagrams using our pipeline.

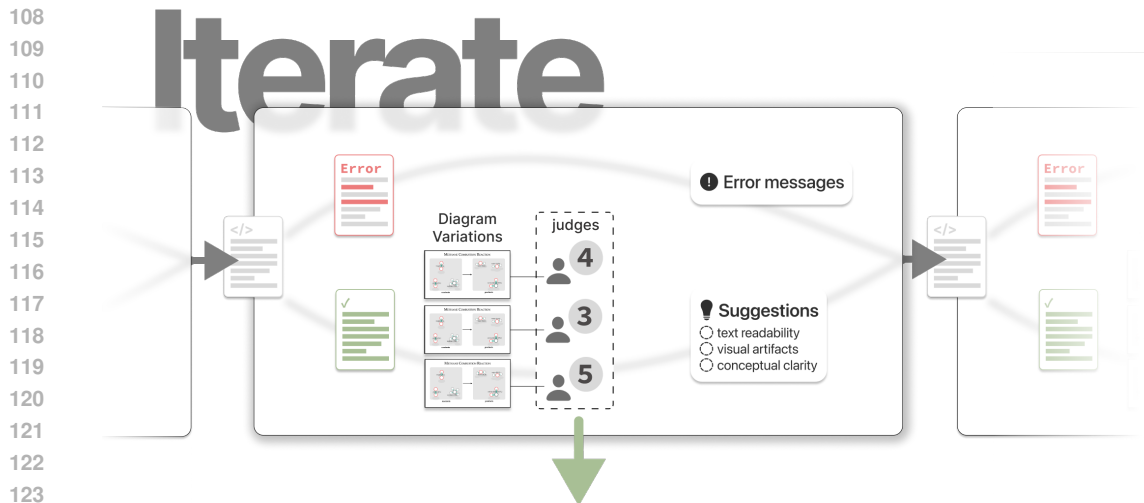


Figure 3: **Iterate Step**: At each step, FEYNMAN attempts to write PENROSE program to create a diagram. The generated program is then compiled into images and sent to a panel of visual judges (MLLMs) for critical feedback. We term this algorithm **Iterative Visual-Refine** (Algorithm 1).

Among prior work that explored similar directions, Belouadi et al. (2023) and Belouadi et al. (2024a) collected datasets of TikZ diagrams from the internet and arXiv articles to train coding agents for TikZ programs. AUTOMATIKZ (Belouadi et al., 2023) is an LLM coding agent that writes TikZ programs given text captions. However, after being trained with hundreds of thousands of TikZ diagrams scraped from arXiv L^AT_EX sources, AUTOMATIKZ still exhibits efficiency overhead in synthesizing scientific diagrams at scale, due to the inherent complexity of both the TikZ language and visual design. In fact, both Belouadi et al. (2023) and Belouadi et al. (2024a) requires time-consuming tree search to boost compile success rates for simple programs, making large-scale generation infeasible. In general, there is still a lack of economical and scalable solution for generating diagrams embedded with rich knowledge.

2 DIAGRAMMING AGENT PIPELINE

In this section, we present the workflow of our diagramming agent, FEYNMAN. FEYNMAN’s diagram synthesis pipeline includes four steps: **idea**, **plan**, **iterate**, and **render**. By leveraging the knowledge capacity of LLMs and a conceptual diagramming tool, FEYNMAN can generate grounded and diverse visual representations of scientific concepts at scale. Our pipeline has the following characteristics:

1. *Knowledge scalability*: Our choice to use an LLM to provide general “knowledge-focused planning” decouples the domain knowledge elicitation and the domain-specific visual design. This choice alleviates the cost of obtaining diverse and high-quality knowledge for the generation of domain-specific diagrams (Section 2.2).
2. *Visual diversity*: The optimization-based approach of the PENROSE rendering engine provides visual diversity even given the same visual concept (Section 2.1), boosting visual diversity of the synthesized diagrams.
3. *Image-text alignment*: The programs written by FEYNMAN simply encode the conceptual ideas and relationships, from which the visuals are automatically derived. These programs resemble natural language descriptions of the concepts, enabling smooth translation between concepts and code.

In this section, we first present the background of conceptual diagramming, which is the foundation of our approach, and then introduce each step in the agentic pipeline of FEYNMAN.

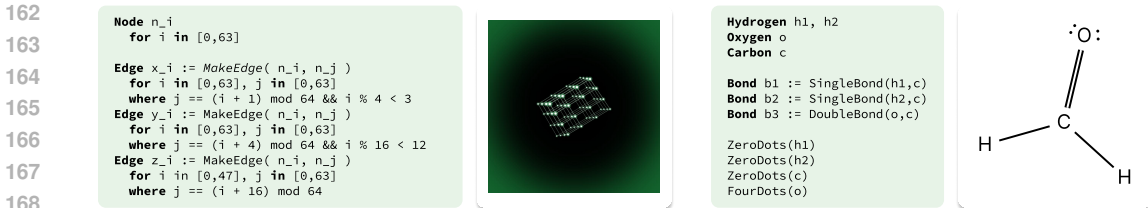


Figure 4: **Examples of conceptual diagrams and their Substance notations:** a graph where node connections form a cube (left) and the Lewis structure of the formaldehyde molecule (CH_2O).

2.1 BACKGROUND: CONCEPTUAL DIAGRAMMING

Conceptual diagrams refer to abstract images that visually represent “a set of ideas and their relations” (Tversky, 2017). At present, most conceptual diagrams are created by either a drawing tool like Adobe Illustrator or a low-level graphical programming language like PGF/TikZ or SVG. Using these tools is highly manual and it is extremely difficult to use them to automating diagram production (Ma’ayan & Ni et al., 2020). As a result, AI generation of diagrams through TikZ has proved challenging (Belouadi et al., 2023) (Fig. 7).

PENROSE is a diagramming tool specifically targeting conceptual diagrams. PENROSE separates the abstract concepts in the diagram (the Substance) and the visual representations of said concepts (the Style). Substance contains no low-level visual details, it is simpler and easier to generate correctly (Fig. 4). Style defines a diverse space of *diagram variations* for any given Substance. Combining Substance and Style, PENROSE samples from this space when rendering a diagram, providing FEYNMAN the ability to produce many different examples even from just one set of concepts (Fig. 6).

To translate from concepts to visuals, Style converts the concepts and relationships from Substance into a constrained optimization problem: every concept in substance is translated to one or more shapes $\mathcal{S} = \{S_1, \dots, S_n\}$, each with degrees of freedom $\vec{p} = (p_1, \dots, p_m)$ such as width, height, and center. Conceptual relations among concepts are translated to *constraints* and *objectives*: constraints ensure that geometric predicates (e.g., contains, disjoint, etc.) hold true, while objectives encourage geometric relations to hold in the resulting diagram (e.g., shapes should be as far apart as possible). PENROSE encodes constraints as nonnegative penalty functions $\mathcal{P}_1, \dots, \mathcal{P}_l : \mathbb{R}^m \rightarrow \mathbb{R}_{\geq 0}$ each of which equal 0 if and only if the constraint is satisfied. Objectives are energy terms $\mathcal{E}_1, \dots, \mathcal{E}_k$. Overall, the PENROSE layout engine solves an optimization problem:

$$\min_{\vec{p} \in \mathbb{R}^m} \sum_{i=1}^k \mathcal{E}_i(\vec{p}) \quad \text{s.t.} \quad \sum_{i=1}^l \mathcal{P}_i(\vec{p}) = 0. \quad (1)$$

PENROSE employs an exterior point method (Hiroshi & Tanabe, 2010) to pose this problem as a sequence of unconstrained optimization problems, where constraints are iteratively stiffened over layout steps:

$$\min_{\vec{p} \in \mathbb{R}^m} \sum_{i=1}^k \mathcal{E}_i(\vec{p}) + c_n \sum_{i=1}^l \mathcal{P}_i^2(\vec{p}), \quad n = 0, 1, 2, \dots \quad (2)$$

PENROSE solve this layout problem by running L-BFGS with line search (Lewis & Overton, 2009).

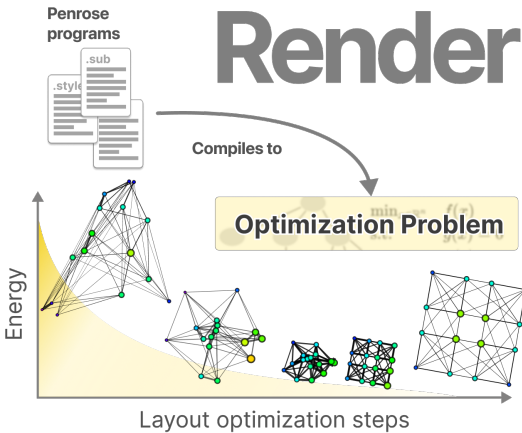


Figure 5: FEYNMAN generates programs that PENROSE compiles to generate an layout optimization problem. The PENROSE layout engine then solves the optimization problem.

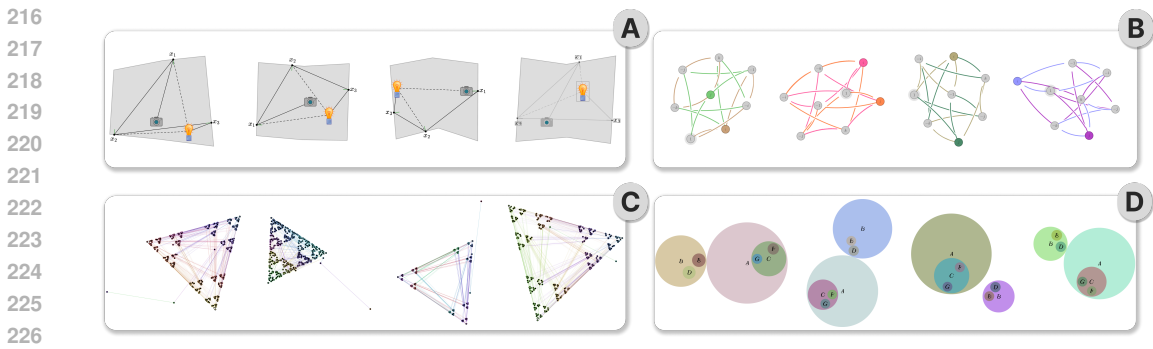


Figure 6: **Diverse visual layouts of PENROSE diagram variations:** using the same Substance, PENROSE can produce diagram variations while preserving the semantics, by sampling random initial values for shapes, colors, and other numerical quantities in the diagram. We show 4 random seed for 4 Substance programs for (A) ray-tracing diagrams, (B) Cayley graphs, (C) Chaos game as a Sierpinski triangle, and (D) Euler diagrams for sets.

2.2 KNOWLEDGE PLANNING: ENUMERATING THE DOMAIN KNOWLEDGE WITH AN LLM

State-of-the-art LLMs learn vast knowledge during their large-scale pretraining. For example, GPT-4o attains 53% accuracy in the GPQA benchmark (Rein et al., 2023), close to the 57% achieved by human experts who have or are pursuing Ph.D. degrees. We leverage this large capacity of knowledge of LLM by designing domain-specific prompts to ask an LLM to enumerate pieces of knowledge (“ideas”) related to the selected domain. The prompts are designed to encourage LLM to perform creative knowledge enumeration. For example, LLM is given the question “Enumerate N chemical reactions that are pedagogical and important.” in the chemical-reactions domain (see examples of full domain planning prompts in Appendix B.2). We feed the LLM’s response to the coding agent, FEYNMAN, to program the concepts into diagrams. In cases where we can’t parse the output format, we try multiple rounds until we reach a maximum number of rounds.

2.3 DIAGRAMMING CODE PLANNING: REASONING FOR CONCEPTUAL DIAGRAMMING

In this stage, the FEYNMAN agent generates a coding plan for each of proposed knowledge components. The agent first attempts to organize the knowledge components into visual concepts, aiming to prepare for translation into PENROSE code. To make the FEYNMAN agent aware of the PENROSE syntax, we provide the official PENROSE documentation in the prompt, akin to Wu et al. (2024a). Moreover, for each domain, we provide a few in-context examples for LLM to learn the syntax for that specific domain. We then instruct FEYNMAN to plan the visual elements that are described in each knowledge component. This involves listing important steps to write a Substance program that corresponds to the sampled knowledge component (see full code planning prompts in Appendix B.4). Note that *we do not instruct the model to write runnable code in this step*, which is an explicit design choice. In Section 4, we show that they serve as crucial foundations for successful and diverse code generation.

2.4 ITERATIVE VISUAL-REFINE WITH A PANEL OF VISUAL JUDGES

After the planning stage, FEYNMAN translates the plan into compilable and correct PENROSE programs. We found in our preliminary experiments that even though LLMs such as GPT-4o fail to write the correct program in their first attempt, they can improve if given suitable suggestions in multi-round conversations. This is close to the **interactive self-refine** approach (Madaan et al., 2024), which improves LLM output quality via multi-round self-reflection. The refinement of diagrams, which involves visual judgments, posed different challenges. While the prior work adopt tree search to perform refinement (Belouadi et al., 2023; 2024a), their refinement process primarily aims to achieve better compilation success rate. Without visual judgments and feedback, the generated visual artifacts might include incorrect representation of knowledge.

To address this challenge, FEYNMAN utilizes a panel of visual judges to provide the visual feedback, which we term it as **Iterative Visual-Refine**. The process is illustrated in Figure 3. In the first round, FEYNMAN receives the plans from the previous planning steps and attempts to generate the first code sample. If the code is successfully compiled into a diagram, then FEYNMAN run PENROSE to generate variations of this diagram and send them to a panel of *visual judges* to assess its quality. Each visual judge is a vision-language model asked to provide critical feedback to the diagramming agent based on a set of *criteria* on various aspects of diagram qualities. To keep the task simple, we prompt the judges to answer in boolean values, which are then collected and aggregated. For cost-saving purposes, we set a threshold of scores above which we accepts the output as a valid diagram. We provide an aggregated feedback message and move to the next iteration if the program generated arrives at any of these states: a) cannot be extracted from the LLM response; b) fail to compile to diagrams or c) receive scores below the set threshold. The formal algorithm is presented in Algorithm 1.

De-duplication. LLM sometimes duplicate their responses given similar prompts, resulting in a lack of diversity of knowledge in diagrams. Specifically, we focus on de-duplicating the Substance code, which PENROSE uses to synthesize diagrams. We use a statement-wise Levenshtein distance (Levenshtein, 1966) to filter programs that contain too many duplicate statements. The detail is presented in Appendix B.6.

2.5 GROUNDED QUESTION-ANSWER PAIR GENERATION

For each Substance code FEYNMAN generated, we generate grounded captions from their code programs, while diversifying its visual representation through the PENROSE optimization-based layout engine. We created a multiple-choice question-answering (QA) data generation pipeline. First, we generate image captions by translating the concepts and relations in Substance to natural language. Then, we prompt an LLM to select one of five visual reasoning skill categories (Appendix B.7) for the problem. To ensure problem diversity and quality, we ask the model to provide rationales before QA generation in a chain-of-thought fashion. Finally, after a QA pair is generated, the model self-verify by checking if the question can be answered without an image and if the answer is correct given both image and question.

2.6 BENCHMARK CURATION: THE DIAGRAMMA BENCHMARK

We curated DIAGRAMMA, a visual reasoning benchmark using diagrams FEYNMAN synthesized. These diagrams are completely unseen and do not exist on the internet. DIAGRAMMA is a scientific benchmark that contains **1,058** multiple choice questions of visual understanding and reasoning. We manually filtered a synthetic test dataset generated by FEYNMAN to create DIAGRAMMA. We went through a meticulous filtering process to ensure that the selected images had accurate labels, correct knowledge representation, and sufficiently challenging questions. As shown in Table 1, DIAGRAMMA contains 6 subjects, each of which contains multiple subdomains e.g., sorting algorithms in computer science. Diagram counts for all subjects are listed in Table 2.

Algorithm 1 Iterative Visual-Refine

Require: Prompt S , Maximum iterations N_{\max} , Quality threshold θ , Number of Judges K

- 1: **Initial Message:** $S_0 \leftarrow S$
- 2: $n \leftarrow 0$ {Initialize iteration counter}
- 3: **while** $n \leq N_{\max}$ **do**
- 4: Agent response $R \leftarrow \text{FEYNMAN}(S)$
- 5: Parse R into PENROSE program C
- 6: **if** Parsing returns no program **then**
- 7: **continue**
- 8: Compile C to diagrams $d_k, \forall k \in [K]$
- 9: **if** Compilation Failure **then**
- 10: **Error:** $e \leftarrow$ error traceback
- 11: **Message:** $S \leftarrow e$
- 12: **continue**
- 13: **for each** $k \in [K]$ **do**
- 14: **Scoring:** $s^{(k)} \leftarrow V_k(d_k)$
- 15: **Suggestions:** $S^{(k)} \leftarrow V_k(d_k)$
- 16: **Average scores:** $s_{n+1} \leftarrow \text{Avg}(s^{(k)})$
- 17: **Average suggestions:** $S_{n+1} \leftarrow \text{Avg}(S^{(k)})$
- 18: **if** $s_{n+1} \geq \theta$ **then**
- 19: **Exit the algorithm, returns** C
- 20: $n \leftarrow n + 1$
- 21: **return** C

324
325
326
327
328
329
330
331
332
333
334
335
336
337
338
339
340
341
342
343
344
345
346
347
348
349
350
351
352
353
354
355
356
357
358
359
360
361
362
363
364
365
366
367
368
369
370
371
372
373
374
375
376
377

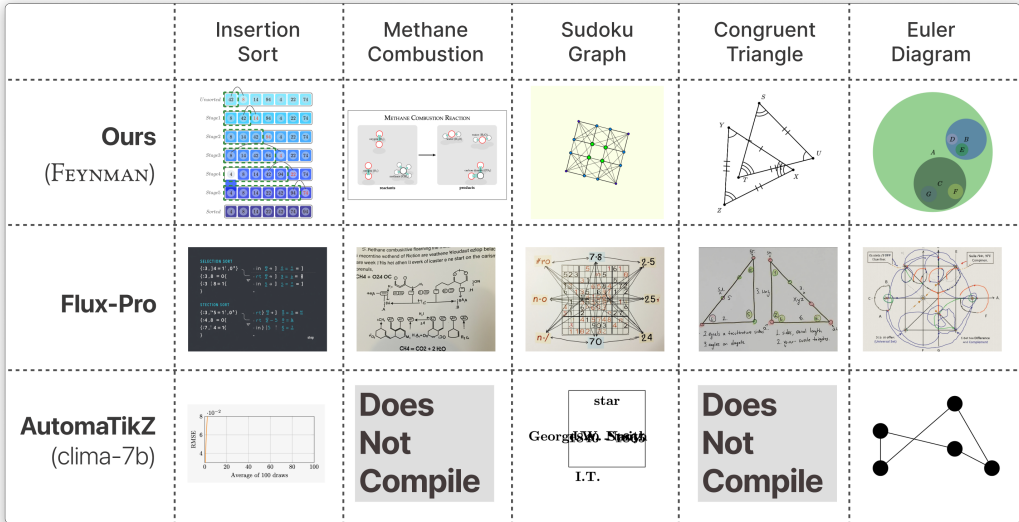


Figure 7: **Comparison of different diagramming approaches:** We select the best image out of three attempts using Flux-Pro and AUTOMATIKZ, compared with those generated by our agent. We provide them with the same prompt for each column. Flux-Pro produces visually diverse diagrams, however none of them contains legible text that matches the intent. AutomaTikZ, on the other hand, only successfully compiled for 3 out of 5 of all prompts.

3 EXPERIMENTS

3.1 SCALING DIAGRAM-CAPTION PAIRS

With the FEYNMAN agent, we conduct a preliminary dataset scaling experiment. By effectively enumerating knowledge in each subject and their subdomains, FEYNMAN produced 10693 unique Substance programs, representing diverse conceptual relationships. We used a total of 1470.4 million input tokens and 46.6 million output tokens on GPT-4o-mini to generate these Substance programs. Each program is further independently rendered by the optimization-based layout engine to produce 10 unique variations, resulting in overall 106930 diagrams. See Figure 6 for examples of diagram variations and their visual diversity. For each rendered variation, we further produce a caption according to both the image and the corresponding Substance program. The scalability of the pipeline is tested in this experiment. In Appendix D.3, we provide more detailed studies to assess the knowledge and visual diversity of generated images.

3.2 DIAGRAMMA EVALUATION

We evaluated DIAGRAMMA on state-of-the-art open- and closed-source MLLMs. Evaluations were conducted in a zero-shot setting, with a uniform template provided to each model. Detailed evaluation setup can be found in Appendix C.

Results. We present the evaluation results of DIAGRAMMA for a set of 17 models in Table 2. We observe three pieces of evidence validating our benchmark curation in the results: 1) as the sizes of models increase, their accuracy consistently improves, confirming the validity of our data for measuring the capabilities of MLLMs; 2) the computer science subject, which primarily involves graph

Source metadata	
Subdomain	108
Substance	1058
Subjects	
Math	401 (37.9%)
CS	342 (32.3%)
Science	241 (22.8%)
Chart	30 (2.8%)
Common Sense	22 (2.1%)
Statistics	22 (2.1%)
Unique Style	52
Unique Domain	38

Table 1: Metadata of DIAGRAMMA.

Model Name	All	Math	CS	Science	Chart	Commonsense	Statistics
Claude-3.5-Sonnet	59.64	64.59	42.98	74.69	53.33	77.27	54.55
GPT-4o (OpenAI (2024a))	57.28	63.09	50.58	60.17	53.33	50.00	36.36
Claude3-Opus (Anthropic (2024))	49.15	54.11	40.35	55.60	33.33	45.45	50.00
Gemini-1.5-Flash (Reid et al. (2024))	47.54	55.36	40.06	45.64	50.00	54.55	31.82
Claude3-Sonnet (Anthropic (2024))	47.54	50.62	38.01	58.92	46.67	36.36	27.27
GPT-4o-mini (OpenAI (2024a))	44.42	47.63	36.55	53.53	26.67	45.45	31.82
Gemini-1.5-pro (Reid et al. (2024))	44.23	49.13	41.23	42.74	30.00	59.09	22.73
Claude3-Haiku (Anthropic (2024))	42.53	46.63	31.58	54.77	30.00	36.36	27.27
Qwen2-VL-72B* (Yang et al. (2024a))	50.85	59.10	42.69	51.45	46.67	31.82	45.45
LLama3.2-VL-90B* (Dubey et al. (2024b))	46.88	50.37	41.23	53.53	26.67	40.91	31.82
LLama3.2-VL-11B (Dubey et al. (2024b))	46.22	48.38	40.06	56.02	30.00	50.00	13.64
Pixtral-12b*	44.71	50.62	40.06	44.81	43.33	36.36	18.18
LLava-OneVision-Qwen2-7b (Li et al. (2024b))	42.91	48.13	35.38	44.40	53.33	45.45	31.82
Qwen2-vl-7B (Yang et al. (2024a))	42.16	48.63	35.38	40.66	43.33	45.45	40.91
InternVL2-8B (Chen et al. (2024))	41.02	47.38	35.09	39.83	40.00	40.91	31.82
Phi-VL-3.5 (Abdin et al. (2024))	38.19	42.64	33.04	40.66	30.00	40.91	18.18
Minicpm-2.6 (Yao et al. (2024))	35.44	41.65	29.82	36.51	26.67	27.27	18.18

Table 2: Accuracy results of DIAGRAMMA on state-of-the-art MLLMs on 1058 samples. Models marked with (*) are evaluated through the OpenRouter API. **Claude-3.5-Sonnet** achieved the highest overall accuracy, with notable performance on science and commonsense diagrams.

reasoning, remains the most difficult for current models, which corroborates with the observations by Li et al. (2024d); Rahmzadehgervi et al. (2024). An notable observation is that Gemini-1.5 Flash, which is considerably cheaper than Gemini-1.5 Pro outperformed Gemini-1.5 Pro on DIAGRAMMA, a trend also seen in the reasoning category in LIVEBENCH (White et al., 2024). We conjecture this correlation is attributed to that DIAGRAMMA share the same “freshness” as the reasoning questions in LIVEBENCH. We find that Gemini 1.5 Pro declined to answer over 100 questions, contributing to a more than 10% drop in accuracy, which might indicates high rejection rates of answering out-of-distribution questions. In Appendix C.4, we present a qualitative analysis of how most MLLMs struggled in reasoning.

4 ANALYSIS

4.1 BASELINE COMPARISON

We show in Figure 7 a preliminary comparison study on 5 attempts to generate diagrams corresponding to specific prompts. We compare FEYNMAN to two competitors AUTOMATIKZ and diffusion model FLUX-Pro (fal.ai, 2024) as baselines. Each attempt of baseline was ran 3 times and we select the best result. The caption is provided in Appendix E.2. The diffusion model FLUX-Pro has difficulty generating clean scientific diagrams that conveys the concepts, but instead hallucinates many low-level details not mentioned in the caption. AUTOMATIKZ (Belouadi et al., 2023), which trained a Llama-2 model to generate TikZ code, fails to produce correct TikZ programs that match the captions. We hypothesize that their failure in our setting if because 1) complex diagrams require great precision to draw than natural images, and 2) TikZ programs cannot separate knowledge organization and visual production, which made the code synthesis task overly difficult. We provide further explorations of using o1-mini and o1-preview (OpenAI, 2024b) to generate TikZ code in Appendix E.2. However, even when powerful LLMs like o1-preview can write TikZ code roughly correctly, TikZ still makes it hard to diversify the layout.

4.2 PRODUCTION-TO-SCALE ANALYSIS

We conducted an ablation experiment shown in Fig. 8 highlights the scalability of FEYNMAN. In knowledge-dense domains, the agent scales its knowledge linearly as the number of tokens increases. Even in knowledge-sparse domains, we observe an upward trend in token generation, though at a reduced rate. This demonstrates the robustness of FEYNMAN’s performance across varying levels of domain.

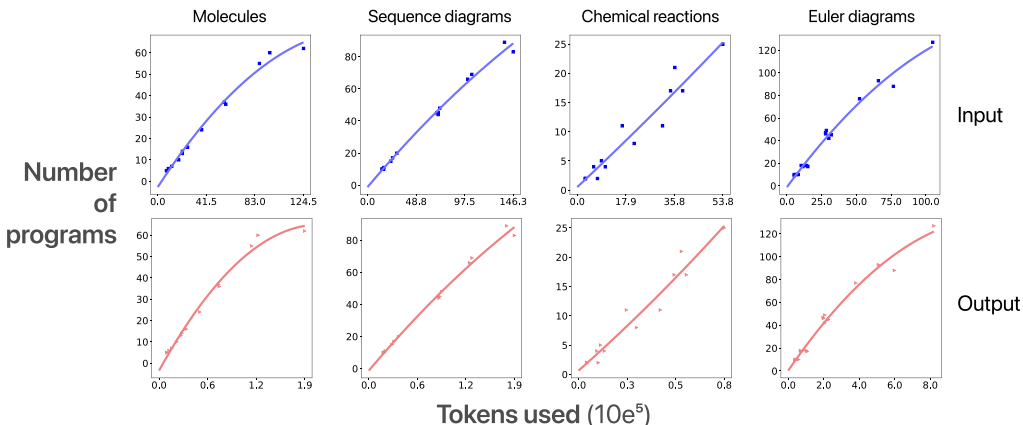


Figure 8: Scaling behavior of input/output tokens versus generated image samples across four subdomains. The figure illustrates two distinct trends: linear scaling in knowledge-dense domains, and decaying trends in knowledge-sparse domains. These trends highlight the impact of domain knowledge diversity and scalability on the performance of FEYNMAN.

The results of our production-to-scale experiment on four selected subdomains are illustrated in Fig. 8. The plots show the total input/output tokens versus the number of generated images after de-duplication. Across the domains, we observe two distinct scaling patterns: a linear trend and a decaying trend. The linear trend suggests the potential for further scaling within a specific domain as the number of tokens increases further. In contrast, the decaying trend indicates diminishing returns in the generation of images as token counts continue to rise. We attribute these differing trends to two main factors: (1) the base model’s knowledge within the specific domain, and (2) the scalability of the domain for diagramming. Additionally, domains can be classified as either knowledge-dense or knowledge-sparse: for instance, enumerating knowledge about chemical reactions is likely easier than for a domain composed solely of complementary triangles.

4.3 ABLATIONS FOR AGENT WORKFLOW

To provide quantitative insights into the effectiveness of FEYNMAN, we evaluate our pipeline on two metrics: the **final yield rate** is percentage of successfully compiled images after de-duplication; the **visual judge scores** is an average of rule-based critic score given by MLLM judges for de-duplicated images at the end of the generation. We perform an ablation study on 10 subdomains that encompass wide range of knowledge. As shown in Table 3, we ablate key components of FEYNMAN: (1) explicit knowledge planing (**KP**, Section 2.2), (2) explicit code planning (**CP**, Section 2.3), and (3) early stop mechanism based on judge scores (**S**, Section 2.4).

We discuss three notable findings from our ablation results. First, the pipeline with all components (**KP + CP + S**) achieves the best average judge score. Second, code planning (**CP**), together with use score to early stop, helps the generation pipeline end in much lower number of rollout rounds. Finally, when knowledge planning (**KP**) is present, the gap between compiled success rate and final yield rate is very low. The observations above suggest that knowledge planning (**KP**) is essential for generating diverse scientific diagrams. Additionally, code planning (**CP**) improves the scalability of the data generation pipeline. When combined with early-stop, **CP** helps generate better-quality figures with fewer iterations and reduce the overall cost. Combing both steps achieves our goal of generating *scalable* and *diverse* diagrams.

5 RELATED WORK

Multi-modal LLMs and agents Vision-language models (Alayrac et al., 2022; Yang et al., 2023; Li et al., 2023a; Zhu et al., 2023) gained remarkable capability of following instructions through visual instruction tuning (Li et al., 2022; Liu et al., 2024b;a). This capability enabled wide range of applications, such as visual reasoning (Yue et al., 2024; Lu et al., 2023), and interact with human as

Ablations	Avg	PR	LT	SP	NR	CR	Compile %	Yield %	Rounds
KP + CP + S	65.4	69.7	30.9	60.4	91.8	74.2	82.5	82.5	2.63
CP + S	65.0	65.9	32.1	59.9	95.0	72.2	97.0	87.5	2.44
KP + S	62.8	63.9	35.6	56.8	91.3	66.2	87.0	86.5	6.69
S	63.2	64.3	31.5	57.6	90.6	71.8	96.5	84.0	6.29
KP + CP	61.5	67.9	25.9	52.1	89.7	71.9	81.5	81.5	8.00
CP	61.8	69.3	23.6	52.5	92.3	71.1	96.5	92.5	8.00
KP	63.9	66.6	32.1	59.5	91.2	70.2	87.5	87.5	8.00

Table 3: The table shows a break down of critic scores in five categories (see Appendix D.1, **PR**: proper element relationship; **LT**: legible text; **NR**: non-redundancy; **CR**: correct representation; **SP**: simplicity), diagram compilation rate (**Compile %**), final yield rate (**Yield %**), and total number of rounds in the iterate step (**Rounds**). The combination of explicit knowledge planning (**KP**), code planning (**CP**), and early stop based on scoring results (**S**) received the best judge critic score.

visual chatbots OpenAI (2024a). Meanwhile, agents built with LLMs can interact with environments (Wang et al., 2024c) to play games, perform web navigation, and write computer programs (Wang et al., 2023; Yao et al., 2022; Romera-Paredes et al., 2024; Yang et al., 2024c; Xia et al., 2024; Wu et al., 2024b). MLLM agents have more perception modalities and are more grounded in real-world scenarios (Hong et al., 2024; Sun et al., 2022; Li et al., 2024a; Wang et al., 2024a; Bonatti et al., 2024; Koh et al., 2024; Li et al., 2024e). Agents are also important collectors of data, but the efficiency of data collection depends on the domain of choice (Putta et al., 2024).

Synthetic data generation The success of large AI models depends primarily on the scaling law of model size and training data (Kaplan et al., 2020; Hoffmann et al., 2022), which stimulated efforts to curate datasets (Gao et al., 2020; Soboleva et al., 2023; Li et al., 2024c). For domains where data collection is expensive, synthesizing data has become the dominant approach (Haluptzok et al., 2022; Zelikman et al., 2022; Yang et al., 2024b; Li et al., 2023b; Wang et al., 2022; Peng et al., 2023). Synthetic data have long existed in the vision domain (Little & Verri, 1989). For multi-modal AI models, teaching the model to harness their visual reasoning capabilities also relies on synthetic data (Li et al., 2022; Liu et al., 2024b;a). One work that tackled similar problems to ours is by Zhang et al. (2024b), who synthesized charts and figures via LLM knowledge and program synthesis, but their approach is limited by the tool of choice and lack of agentic ability such as iterative refinement.

Vision-language benchmarks Sustainable progress of AI research relies on the continuous development of benchmarks to measure the capabilities of AI systems. Benchmarks like HellaSwag (Zellers et al., 2019; Hendrycks et al., 2020; Cobbe et al., 2021; Zheng et al., 2023) contributed significantly to the progress measurement of building state-of-the-art LLMs. Vision-language benchmarks serve the same role for the visual understanding and reasoning abilities of MLLMs. For example, benchmarks like VQA-v2 (Antol et al., 2015), GQA (Hudson & Manning, 2019) and MMMU (Yue et al., 2024) measure the visual knowledge of MLLMs comprehensively. Other benchmarks like (Methani et al., 2020; Lu et al., 2021b;a; Masry et al., 2022; Lu et al., 2024; Wang et al., 2024b) measure domain-specific capabilities like chart understanding and math visual reasoning.

6 CONCLUSION

In this paper, we presented FEYNMAN, a diagramming agent that authors conceptual diagrams at scale. FEYNMAN decouples knowledge elicitation from visual production of diagrams to achieve scalability of diagram synthesis. Grounded by a knowledge-infused diagramming language, FEYNMAN produces text-image pairs to scale up the synthetic data across multiple subjects, such as computer science and mathematics. We conducted systematic ablation of key design choices for FEYNMAN, and showed the production-to-scale curves to demonstrate the scalability of our pipeline. Additionally, we released a new benchmark DIAGRAMMA with question-answer pairs generated by FEYNMAN and curated to ensure correctness, further contributing to research in diagram-based reasoning.

REFERENCES

- 540
541
542 Marah Abdin, Sam Ade Jacobs, Ammar Ahmad Awan, Jyoti Aneja, Ahmed Awadallah, Hany
543 Awadalla, Nguyen Bach, Amit Bahree, Arash Bakhtiari, Harkirat Behl, et al. Phi-3 technical re-
544 port: A highly capable language model locally on your phone. *arXiv preprint arXiv:2404.14219*,
545 2024.
- 546 Jean-Baptiste Alayrac, Jeff Donahue, Pauline Luc, Antoine Miech, Iain Barr, Yana Hasson, Karel
547 Lenc, Arthur Mensch, Katherine Millican, Malcolm Reynolds, et al. Flamingo: a visual language
548 model for few-shot learning. *Advances in neural information processing systems*, 35:23716–
549 23736, 2022.
- 550 Anthropic. The claude 3 model family: Opus, sonnet, haiku. 2024. URL https://www-cdn.anthropic.com/de8ba9b01c9ab7cbabf5c33b80b7bbc618857627/Model_Card_Claude_3.pdf.
- 551
552
553 Stanislaw Antol, Aishwarya Agrawal, Jiasen Lu, Margaret Mitchell, Dhruv Batra, C Lawrence Zit-
554 nick, and Devi Parikh. Vqa: Visual question answering. In *Proceedings of the IEEE international*
555 *conference on computer vision*, pp. 2425–2433, 2015.
- 556
557 Jonas Belouadi, Anne Lauscher, and Steffen Eger. Automatizk: Text-guided synthesis of scientific
558 vector graphics with tikz. *arXiv preprint arXiv:2310.00367*, 2023.
- 559
560 Jonas Belouadi, Steffen Eger, and Simone Paolo Ponzetto. Detikzify: Synthesizing graphics pro-
561 grams for scientific figures and sketches with tikz. *arXiv preprint arXiv:2405.15306*, 2024a.
- 562
563 Jonas Belouadi, Anne Lauscher, and Steffen Eger. AutomaTikZ: Text-Guided Synthesis of Scientific
564 Vector Graphics with TikZ, 2024b. arXiv: cs.CL/2310.00367.
- 565
566 Jonas Belouadi, Simone Paolo Ponzetto, and Steffen Eger. DeTikZify: Synthesizing Graphics Pro-
567 grams for Scientific Figures and Sketches with TikZ, May 2024c. URL <http://arxiv.org/abs/2405.15306>. arXiv:2405.15306 [cs].
- 568
569 Rogerio Bonatti, Dan Zhao, Francesco Bonacci, Dillon Dupont, Sara Abdali, Yinheng Li, Justin Wa-
570 ggle, Kazuhito Koishida, Arthur Buckner, Lawrence Jang, et al. Windows agent arena: Evaluating
571 multi-modal os agents at scale. *arXiv preprint arXiv:2409.08264*, 2024.
- 572
573 Zhe Chen, Weiyun Wang, Hao Tian, Shenglong Ye, Zhangwei Gao, Erfei Cui, Wenwen Tong,
574 Kongzhi Hu, Jiapeng Luo, Zheng Ma, et al. How far are we to gpt-4v? closing the gap to com-
575 mercial multimodal models with open-source suites. *arXiv preprint arXiv:2404.16821*, 2024.
- 576
577 Karl Cobbe, Vineet Kosaraju, Mohammad Bavarian, Mark Chen, Heewoo Jun, Lukasz Kaiser,
578 Matthias Plappert, Jerry Tworek, Jacob Hilton, Reiichiro Nakano, et al. Training verifiers to
579 solve math word problems. *arXiv preprint arXiv:2110.14168*, 2021.
- 580
581 Abhimanyu Dubey, Abhinav Jauhri, Abhinav Pandey, Abhishek Kadian, Ahmad Al-Dahle, Aiesha
582 Letman, Akhil Mathur, Alan Schelten, Amy Yang, Angela Fan, et al. The llama 3 herd of models.
583 *arXiv preprint arXiv:2407.21783*, 2024a.
- 584
585 Abhimanyu Dubey, Abhinav Jauhri, Abhinav Pandey, Abhishek Kadian, Ahmad Al-Dahle, Aiesha
586 Letman, Akhil Mathur, Alan Schelten, Amy Yang, Angela Fan, et al. The llama 3 herd of models.
587 *arXiv preprint arXiv:2407.21783*, 2024b.
- 588
589 Aryaz Eghbali and Michael Pradel. Crystalbleu: precisely and efficiently measuring the similarity
590 of code. In *Proceedings of the 37th IEEE/ACM International Conference on Automated Software*
591 *Engineering*, pp. 1–12, 2022.
- 592
593 fal.ai. Flux-pro. <https://fal.ai/models/fal-ai/flux-pro>, 2024.
- Leo Gao, Stella Biderman, Sid Black, Laurence Golding, Travis Hoppe, Charles Foster, Jason Phang, Horace He, Anish Thite, Noa Nabeshima, et al. The pile: An 800gb dataset of diverse text for language modeling. *arXiv preprint arXiv:2101.00027*, 2020.

- 594 Patrick Haluptzok, Matthew Bowers, and Adam Tauman Kalai. Language models can teach them-
595 selves to program better. *arXiv preprint arXiv:2207.14502*, 2022.
596
- 597 Dan Hendrycks, Collin Burns, Steven Basart, Andy Zou, Mantas Mazeika, Dawn Song, and
598 Jacob Steinhardt. Measuring massive multitask language understanding. *arXiv preprint*
599 *arXiv:2009.03300*, 2020.
- 600 Yamashita Hiroshi and Takahito Tanabe. A Primal-Dual Exterior Point Method for Nonlinear
601 Optimization. <http://dx.doi.org/10.1137/060676970>, 20(6):3335–3363, November 2010. ISSN
602 10526234. doi: 10.1137/060676970. URL [https://epubs.siam.org/doi/abs/10.1137/](https://epubs.siam.org/doi/abs/10.1137/060676970)
603 [060676970](https://epubs.siam.org/doi/abs/10.1137/060676970). Publisher: Society for Industrial and Applied Mathematics.
604
- 605 Jordan Hoffmann, Sebastian Borgeaud, Arthur Mensch, Elena Buchatskaya, Trevor Cai, Eliza
606 Rutherford, Diego de Las Casas, Lisa Anne Hendricks, Johannes Welbl, Aidan Clark, et al. Train-
607 ing compute-optimal large language models. *arXiv preprint arXiv:2203.15556*, 2022.
- 608 Wenyi Hong, Weihang Wang, Qingsong Lv, Jiazhen Xu, Wenmeng Yu, Junhui Ji, Yan Wang, Zihan
609 Wang, Yuxiao Dong, Ming Ding, et al. Cogagent: A visual language model for gui agents.
610 In *Proceedings of the IEEE/CVF Conference on Computer Vision and Pattern Recognition*, pp.
611 14281–14290, 2024.
- 612 Drew A Hudson and Christopher D Manning. Gqa: A new dataset for real-world visual reasoning
613 and compositional question answering. In *Proceedings of the IEEE/CVF conference on computer*
614 *vision and pattern recognition*, pp. 6700–6709, 2019.
615
- 616 Jared Kaplan, Sam McCandlish, Tom Henighan, Tom B Brown, Benjamin Chess, Rewon Child,
617 Scott Gray, Alec Radford, Jeffrey Wu, and Dario Amodei. Scaling laws for neural language
618 models. *arXiv preprint arXiv:2001.08361*, 2020.
- 619 Jing Yu Koh, Robert Lo, Lawrence Jang, Vikram Duvvur, Ming Chong Lim, Po-Yu Huang, Graham
620 Neubig, Shuyan Zhou, Ruslan Salakhutdinov, and Daniel Fried. Visualwebarena: Evaluating
621 multimodal agents on realistic visual web tasks. *arXiv preprint arXiv:2401.13649*, 2024.
622
- 623 Jill H. Larkin and Herbert A. Simon. Why a Diagram is (Sometimes) Worth Ten Thou-
624 sand Words. *Cognitive Science*, 11(1):65–100, January 1987. ISSN 0364-0213. doi: 10.
625 1016/S0364-0213(87)80026-5. URL [http://www.sciencedirect.com/science/article/](http://www.sciencedirect.com/science/article/pii/S0364021387800265)
626 [pii/S0364021387800265](http://www.sciencedirect.com/science/article/pii/S0364021387800265).
- 627 V Levenshtein. Binary codes capable of correcting deletions, insertions, and reversals. *Proceedings*
628 *of the Soviet physics doklady*, 1966.
629
- 630 A. S. Lewis and M. L. Overton. Nonsmooth optimization via BFGS. *SIAM J. Optimiz.*, pp. 1–35,
631 2009.
- 632 Binxu Li, Tiankai Yan, Yuanting Pan, Zhe Xu, Jie Luo, Ruiyang Ji, Shilong Liu, Haoyu Dong, Zihao
633 Lin, and Yixin Wang. Mmedagent: Learning to use medical tools with multi-modal agent. *arXiv*
634 *preprint arXiv:2407.02483*, 2024a.
- 635 Bo Li, Yuanhan Zhang, Dong Guo, Renrui Zhang, Feng Li, Hao Zhang, Kaichen Zhang, Yanwei
636 Li, Ziwei Liu, and Chunyuan Li. Llava-onevision: Easy visual task transfer. *arXiv preprint*
637 *arXiv:2408.03326*, 2024b.
638
- 639 Jeffrey Li, Alex Fang, Georgios Smyrnis, Maor Ivgi, Matt Jordan, Samir Gadre, Hritik Bansal,
640 Etash Guha, Sedrick Keh, Kushal Arora, et al. Datacomp-lm: In search of the next generation of
641 training sets for language models. *arXiv preprint arXiv:2406.11794*, 2024c.
- 642 Junnan Li, Dongxu Li, Caiming Xiong, and Steven Hoi. Blip: Bootstrapping language-image pre-
643 training for unified vision-language understanding and generation. In *International conference*
644 *on machine learning*, pp. 12888–12900. PMLR, 2022.
645
- 646 Junnan Li, Dongxu Li, Silvio Savarese, and Steven Hoi. Blip-2: Bootstrapping language-image
647 pre-training with frozen image encoders and large language models. In *International conference*
on machine learning, pp. 19730–19742. PMLR, 2023a.

- 648 Yuanzhi Li, Sébastien Bubeck, Ronen Eldan, Allie Del Giorno, Suriya Gunasekar, and Yin Tat Lee.
649 Textbooks are all you need ii: phi-1.5 technical report. *arXiv preprint arXiv:2309.05463*, 2023b.
650
- 651 Yunxin Li, Baotian Hu, Haoyuan Shi, Wei Wang, Longyue Wang, and Min Zhang. VisionGraph:
652 Leveraging Large Multimodal Models for Graph Theory Problems in Visual Context, May 2024d.
653 URL <https://arxiv.org/abs/2405.04950v1>.
- 654 Zaijing Li, Yuquan Xie, Rui Shao, Gongwei Chen, Dongmei Jiang, and Liqiang Nie. Optimus-
655 1: Hybrid multimodal memory empowered agents excel in long-horizon tasks. *arXiv preprint*
656 *arXiv:2408.03615*, 2024e.
657
- 658 JJ Little and A Verri. Analysis of differential and matching methods for optical flow. In *[1989]*
659 *Proceedings. Workshop on Visual Motion*, pp. 173–180. IEEE, 1989.
- 660 Haotian Liu, Chunyuan Li, Yuheng Li, and Yong Jae Lee. Improved baselines with visual instruction
661 tuning. In *Proceedings of the IEEE/CVF Conference on Computer Vision and Pattern Recogni-*
662 *tion*, pp. 26296–26306, 2024a.
- 663 Haotian Liu, Chunyuan Li, Qingyang Wu, and Yong Jae Lee. Visual instruction tuning. *Advances*
664 *in neural information processing systems*, 36, 2024b.
- 665 Pan Lu, Ran Gong, Shibiao Jiang, Liang Qiu, Siyuan Huang, Xiaodan Liang, and Song-Chun Zhu.
666 Inter-gps: Interpretable geometry problem solving with formal language and symbolic reasoning.
667 *arXiv preprint arXiv:2105.04165*, 2021a.
- 668 Pan Lu, Liang Qiu, Jiaqi Chen, Tony Xia, Yizhou Zhao, Wei Zhang, Zhou Yu, Xiaodan Liang,
669 and Song-Chun Zhu. Iconqa: A new benchmark for abstract diagram understanding and visual
670 language reasoning. *arXiv preprint arXiv:2110.13214*, 2021b.
- 671 Pan Lu, Hritik Bansal, Tony Xia, Jiacheng Liu, Chunyuan Li, Hannaneh Hajishirzi, Hao Cheng, Kai-
672 Wei Chang, Michel Galley, and Jianfeng Gao. Mathvista: Evaluating mathematical reasoning of
673 foundation models in visual contexts. *arXiv preprint arXiv:2310.02255*, 2023.
- 674 Pan Lu, Hritik Bansal, Tony Xia, Jiacheng Liu, Chunyuan Li, Hannaneh Hajishirzi, Hao Cheng, Kai-
675 Wei Chang, Michel Galley, and Jianfeng Gao. MathVista: Evaluating Mathematical Reasoning
676 of Foundation Models in Visual Contexts, January 2024. URL <http://arxiv.org/abs/2310.02255> [cs].
- 677 Dor Ma’ayan, Wode Ni, Katherine Ye, Chinmay Kulkarni, and Joshua Sunshine. How Domain
678 Experts Create Conceptual Diagrams and Implications for Tool Design. *Conference on Human*
679 *Factors in Computing Systems - Proceedings*, 20, April 2020. doi: 10.1145/3313831.3376253.
680 Publisher: Association for Computing Machinery ISBN: 9781450367080.
- 681 Aman Madaan, Niket Tandon, Prakhar Gupta, Skyler Hallinan, Luyu Gao, Sarah Wiegrefe, Uri
682 Alon, Nouha Dziri, Shrimai Prabhumoye, Yiming Yang, et al. Self-refine: Iterative refinement
683 with self-feedback. *Advances in Neural Information Processing Systems*, 36, 2024.
- 684 Ahmed Masry, Do Xuan Long, Jia Qing Tan, Shafiq Joty, and Enamul Hoque. ChartQA: A Bench-
685 mark for Question Answering about Charts with Visual and Logical Reasoning, March 2022.
686 URL <http://arxiv.org/abs/2203.10244>. arXiv:2203.10244 [cs].
- 687 Brandon McKinzie, Zhe Gan, Jean-Philippe Fauconnier, Sam Dodge, Bowen Zhang, Philipp Dufer,
688 Dhruvi Shah, Xianzhi Du, Futang Peng, Floris Weers, Anton Belyi, Haotian Zhang, Karanjeet
689 Singh, Doug Kang, Ankur Jain, Hongyu Hè, Max Schwarzer, Tom Gunter, Xiang Kong, Aonan
690 Zhang, Jianyu Wang, Chong Wang, Nan Du, Tao Lei, Sam Wiseman, Guoli Yin, Mark Lee,
691 Zirui Wang, Ruoming Pang, Peter Grasch, Alexander Toshev, and Yinfei Yang. MM1: Methods,
692 Analysis & Insights from Multimodal LLM Pre-training, April 2024. URL <http://arxiv.org/abs/2403.09611>. arXiv:2403.09611 [cs].
- 693 Nitesh Methani, Pritha Ganguly, Mitesh M Khapra, and Pratyush Kumar. Plotqa: Reasoning over
694 scientific plots. In *Proceedings of the IEEE/CVF Winter Conference on Applications of Computer*
695 *Vision*, pp. 1527–1536, 2020.

- 702 OpenAI. Gpt-4o system card, 2024a. URL <https://openai.com/index/gpt-4o-system-card/>.
703
- 704 OpenAI. Learning to reason with llms, 2024b. URL [https://openai.com/index/](https://openai.com/index/learning-to-reason-with-llms)
705 [learning-to-reason-with-llms](https://openai.com/index/learning-to-reason-with-llms).
706
- 707 Kishore Papineni, Salim Roukos, Todd Ward, and Wei-Jing Zhu. Bleu: a method for automatic
708 evaluation of machine translation. In *Proceedings of the 40th annual meeting of the Association*
709 *for Computational Linguistics*, pp. 311–318, 2002.
- 710 Baolin Peng, Chunyuan Li, Pengcheng He, Michel Galley, and Jianfeng Gao. Instruction tuning
711 with gpt-4. *arXiv preprint arXiv:2304.03277*, 2023.
712
- 713 Pranav Putta, Edmund Mills, Naman Garg, Sumeet Motwani, Chelsea Finn, Divyansh Garg, and
714 Rafael Rafailov. Agent q: Advanced reasoning and learning for autonomous ai agents. *arXiv*
715 *preprint arXiv:2408.07199*, 2024.
- 716 Alec Radford, Jong Wook Kim, Chris Hallacy, Aditya Ramesh, Gabriel Goh, Sandhini Agarwal,
717 Girish Sastry, Amanda Askell, Pamela Mishkin, Jack Clark, et al. Learning transferable visual
718 models from natural language supervision. In *International conference on machine learning*, pp.
719 8748–8763. PMLR, 2021.
- 720 Pooyan Rahmazadehgervi, Logan Bolton, Mohammad Reza Taesiri, and Anh Totti Nguyen.
721 Vision language models are blind, July 2024. URL <http://arxiv.org/abs/2407.06581>.
722 [arXiv:2407.06581](http://arxiv.org/abs/2407.06581) [cs].
723
- 724 Machel Reid, Nikolay Savinov, Denis Teplyashin, Dmitry Lepikhin, Timothy Lillicrap, Jean-
725 baptiste Alayrac, Radu Soricut, Angeliki Lazaridou, Orhan Firat, Julian Schrittwieser, et al. Gem-
726 ini 1.5: Unlocking multimodal understanding across millions of tokens of context. *arXiv preprint*
727 *arXiv:2403.05530*, 2024.
- 728 David Rein, Betty Li Hou, Asa Cooper Stickland, Jackson Petty, Richard Yuanzhe Pang, Julien Di-
729 rani, Julian Michael, and Samuel R Bowman. Gpqa: A graduate-level google-proof q&a bench-
730 mark. *arXiv preprint arXiv:2311.12022*, 2023.
731
- 732 Robin Rombach, Andreas Blattmann, Dominik Lorenz, Patrick Esser, and Björn Ommer. High-
733 resolution image synthesis with latent diffusion models. In *Proceedings of the IEEE/CVF confer-*
734 *ence on computer vision and pattern recognition*, pp. 10684–10695, 2022.
- 735 Bernardino Romera-Paredes, Mohammadamin Barekatin, Alexander Novikov, Matej Balog,
736 M Pawan Kumar, Emilien Dupont, Francisco JR Ruiz, Jordan S Ellenberg, Pengming Wang,
737 Omar Fawzi, et al. Mathematical discoveries from program search with large language models.
738 *Nature*, 625(7995):468–475, 2024.
739
- 740 Daria Soboleva, Faisal Al-Khateeb, Robert Myers, Jacob R Steeves, Joel
741 Hestness, and Nolan Dey. SlimPajama: A 627B token cleaned and
742 deduplicated version of RedPajama. [https://www.cerebras.net/blog/](https://www.cerebras.net/blog/slimpajama-a-627b-token-cleaned-and-deduplicated-version-of-redpajama)
743 [slimpajama-a-627b-token-cleaned-and-deduplicated-version-of-redpajama](https://www.cerebras.net/blog/slimpajama-a-627b-token-cleaned-and-deduplicated-version-of-redpajama), 2023.
744 URL <https://huggingface.co/datasets/cerebras/SlimPajama-627B>.
- 745 Liangtai Sun, Xingyu Chen, Lu Chen, Tianle Dai, Zichen Zhu, and Kai Yu. Meta-gui: Towards
746 multi-modal conversational agents on mobile gui. *arXiv preprint arXiv:2205.11029*, 2022.
747
- 748 Gemini Team, Rohan Anil, Sebastian Borgeaud, Yonghui Wu, Jean-Baptiste Alayrac, Jiahui Yu,
749 Radu Soricut, Johan Schalkwyk, Andrew M Dai, Anja Hauth, et al. Gemini: a family of highly
750 capable multimodal models. *arXiv preprint arXiv:2312.11805*, 2023.
- 751 Shengbang Tong, Ellis Brown, Penghao Wu, Sanghyun Woo, Manoj Middepogu, Sai Charitha
752 Akula, Jihan Yang, Shusheng Yang, Adithya Iyer, Xichen Pan, et al. Cambrian-1: A fully open,
753 vision-centric exploration of multimodal llms. *arXiv preprint arXiv:2406.16860*, 2024.
754
- 755 Barbara Tversky. *Diagrams*. In *Information Design*. Routledge, 2017. ISBN 978-1-315-58568-0.
Num Pages: 12.

- 756 Guanzhi Wang, Yuqi Xie, Yunfan Jiang, Ajay Mandlekar, Chaowei Xiao, Yuke Zhu, Linxi Fan,
757 and Anima Anandkumar. Voyager: An open-ended embodied agent with large language models.
758 *arXiv preprint arXiv:2305.16291*, 2023.
759
- 760 Junyang Wang, Haiyang Xu, Jiabo Ye, Ming Yan, Weizhou Shen, Ji Zhang, Fei Huang, and Jitao
761 Sang. Mobile-agent: Autonomous multi-modal mobile device agent with visual perception. *arXiv*
762 *preprint arXiv:2401.16158*, 2024a.
- 763 Ke Wang, Junting Pan, Weikang Shi, Zimu Lu, Mingjie Zhan, and Hongsheng Li. Measuring
764 multimodal mathematical reasoning with math-vision dataset. *arXiv preprint arXiv:2402.14804*,
765 2024b.
766
- 767 Lei Wang, Chen Ma, Xueyang Feng, Zeyu Zhang, Hao Yang, Jingsen Zhang, Zhiyuan Chen, Jiakai
768 Tang, Xu Chen, Yankai Lin, et al. A survey on large language model based autonomous agents.
769 *Frontiers of Computer Science*, 18(6):186345, 2024c.
- 770 Yizhong Wang, Yeganeh Kordi, Swaroop Mishra, Alisa Liu, Noah A Smith, Daniel Khashabi, and
771 Hannaneh Hajishirzi. Self-instruct: Aligning language models with self-generated instructions.
772 *arXiv preprint arXiv:2212.10560*, 2022.
773
- 774 Colin White, Samuel Dooley, Manley Roberts, Arka Pal, Ben Feuer, Siddhartha Jain, Ravid
775 Shwartz-Ziv, Neel Jain, Khalid Saifullah, Siddhartha Naidu, et al. Livebench: A challenging,
776 contamination-free llm benchmark. *arXiv preprint arXiv:2406.19314*, 2024.
777
- 778 Ronghuan Wu, Wanchao Su, Kede Ma, and Jing Liao. IconShop: Text-Guided Vector Icon Synthesis
779 with Autoregressive Transformers. *ACM Trans. Graph.*, 42(6):230:1–230:14, December 2023.
780 ISSN 0730-0301. doi: 10.1145/3618364. URL <https://dl.acm.org/doi/10.1145/3618364>.
- 781 Yue Wu, Yewen Fan, Paul Pu Liang, Amos Azaria, Yuanzhi Li, and Tom M Mitchell. Read and
782 reap the rewards: Learning to play atari with the help of instruction manuals. *Advances in Neural*
783 *Information Processing Systems*, 36, 2024a.
784
- 785 Yue Wu, Yewen Fan, So Yeon Min, Shrimai Prabhumoye, Stephen McAleer, Yonatan Bisk, Ruslan
786 Salakhutdinov, Yuanzhi Li, and Tom Mitchell. Agentkit: Flow engineering with graphs, not
787 coding. *arXiv preprint arXiv:2404.11483*, 2024b.
- 788 Chunqiu Steven Xia, Yinlin Deng, Soren Dunn, and Lingming Zhang. Agentless: Demystifying
789 llm-based software engineering agents. *arXiv preprint arXiv:2407.01489*, 2024.
790
- 791 An Yang, Baosong Yang, Binyuan Hui, Bo Zheng, Bowen Yu, Chang Zhou, Chengpeng Li,
792 Chengyuan Li, Dayiheng Liu, Fei Huang, et al. Qwen2 technical report. *arXiv preprint*
793 *arXiv:2407.10671*, 2024a.
794
- 795 Jiayi Yang, Binyuan Hui, Min Yang, Jian Yang, Junyang Lin, and Chang Zhou. Synthesizing text-
796 to-sql data from weak and strong llms. *arXiv preprint arXiv:2408.03256*, 2024b.
- 797 John Yang, Carlos E Jimenez, Alexander Wettig, Kilian Lieret, Shunyu Yao, Karthik Narasimhan,
798 and Ofir Press. Swe-agent: Agent-computer interfaces enable automated software engineering.
799 *arXiv preprint arXiv:2405.15793*, 2024c.
800
- 801 Zhengyuan Yang, Linjie Li, Kevin Lin, Jianfeng Wang, Chung-Ching Lin, Zicheng Liu, and Li-
802 juan Wang. The dawn of llms: Preliminary explorations with gpt-4v (ision). *arXiv preprint*
803 *arXiv:2309.17421*, 9(1):1, 2023.
- 804 Shunyu Yao, Howard Chen, John Yang, and Karthik Narasimhan. Webshop: Towards scalable
805 real-world web interaction with grounded language agents. *Advances in Neural Information*
806 *Processing Systems*, 35:20744–20757, 2022.
807
- 808 Yuan Yao, Tianyu Yu, Ao Zhang, Chongyi Wang, Junbo Cui, Hongji Zhu, Tianchi Cai, Haoyu Li,
809 Weilin Zhao, Zhihui He, et al. Minicpm-v: A gpt-4v level mllm on your phone. *arXiv preprint*
arXiv:2408.01800, 2024.

- 810 Katherine Ye, Wode Ni, Max Krieger, Dor Ma’ayan, Jenna Wise, Jonathan Aldrich, Joshua Sun-
811 shine, and Keenan Crane. Penrose: From Mathematical Notation to Beautiful Diagrams. *ACM*
812 *Transactions on Graphics*, 39(4):144:144:1–144:144:16, July 2020. ISSN 0730-0301. doi:
813 10.1145/3386569.3392375. URL <https://doi.org/10.1145/3386569.3392375>.
814
- 815 Xiang Yue, Yuansheng Ni, Kai Zhang, Tianyu Zheng, Ruoqi Liu, Ge Zhang, Samuel Stevens,
816 Dongfu Jiang, Weiming Ren, Yuxuan Sun, et al. Mmmu: A massive multi-discipline multi-
817 modal understanding and reasoning benchmark for expert agi. In *Proceedings of the IEEE/CVF*
818 *Conference on Computer Vision and Pattern Recognition*, pp. 9556–9567, 2024.
- 819 Mert Yuksekgonul, Federico Bianchi, Pratyusha Kalluri, Dan Jurafsky, and James Zou. When and
820 Why Vision-Language Models Behave like Bags-Of-Words, and What to Do About It? Septem-
821 ber 2022. URL <https://openreview.net/forum?id=KRLUvxh8uaX>.
822
- 823 Eric Zelikman, Yuhuai Wu, Jesse Mu, and Noah Goodman. Star: Bootstrapping reasoning with
824 reasoning. *Advances in Neural Information Processing Systems*, 35:15476–15488, 2022.
825
- 826 Rowan Zellers, Ari Holtzman, Yonatan Bisk, Ali Farhadi, and Yejin Choi. Hellaswag: Can a ma-
827 chine really finish your sentence? *arXiv preprint arXiv:1905.07830*, 2019.
- 828 Renrui Zhang, Dongzhi Jiang, Yichi Zhang, Haokun Lin, Ziyu Guo, Pengshuo Qiu, Aojun Zhou,
829 Pan Lu, Kai-Wei Chang, Peng Gao, et al. Mathverse: Does your multi-modal llm truly see the
830 diagrams in visual math problems? *arXiv preprint arXiv:2403.14624*, 2024a.
831
- 832 Wenqi Zhang, Zhenglin Cheng, Yuanyu He, Mengna Wang, Yongliang Shen, Zeqi Tan, Guiyang
833 Hou, Mingqian He, Yanna Ma, Weiming Lu, and Yueting Zhuang. Multimodal Self-Instruct: Syn-
834 thetic Abstract Image and Visual Reasoning Instruction Using Language Model, August 2024b.
835 URL <http://arxiv.org/abs/2407.07053>. arXiv:2407.07053 [cs].
836
- 837 Lianmin Zheng, Wei-Lin Chiang, Ying Sheng, Siyuan Zhuang, Zhanghao Wu, Yonghao Zhuang,
838 Zi Lin, Zhuohan Li, Dacheng Li, Eric Xing, et al. Judging llm-as-a-judge with mt-bench and
839 chatbot arena. *Advances in Neural Information Processing Systems*, 36:46595–46623, 2023.
- 840 Deyao Zhu, Jun Chen, Xiaoqian Shen, Xiang Li, and Mohamed Elhoseiny. Minigt-4: En-
841 hancing vision-language understanding with advanced large language models. *arXiv preprint*
842 *arXiv:2304.10592*, 2023.
843
844

845 A LIMITATION AND FUTURE WORK

847 **Dependency on Implicit Knowledge:** FEYNMAN relies heavily on the implicit knowledge embed-
848 ded in large language models (LLMs) during knowledge elicitation. This reliance can reduce the
849 model’s effectiveness in domains where LLMs have incomplete or biased knowledge, resulting in
850 less diverse outputs. A key area for future work is improving how knowledge is elicited from LLMs.
851 For example, this may involve integrating a Retrieval-Augmented Generation (RAG) pipeline to
852 supplement LLMs with external, domain-specific information.

853 **Limited Diagram Style Variation:** While the generated diagrams exhibit layout diversity, control
854 over stylistic elements, such as color schemes or visual aesthetics, is limited to the default capabil-
855 ities of the PENROSE language. To address this, future efforts will focus on systematically varying
856 Style and Domain programs in PENROSE, enabling more flexible and customizable diagram gener-
857 ation.

859 B DETAILED PIPELINE FOR FEYNMAN

861 B.1 PIPELINE CONFIGURATION

862 Below we create a list of hyperparameters used in FEYNMAN. An ablation study is done in Section 4
863 on some key hyperparameters, labeled with (*).

- 864 • **Planning LLM**: the model used during Knowledge Planning section
- 865 • **Coding LLM**: the model used during Code Planning and Generation
- 866 • **Number of Rounds**: The number of iterative improvement rounds per sample
- 867 • **Critic MLLMs**: a list of MLLM candidate used to judge the image at the end of each
- 868 rollout rounds and final generation pipeline
- 869 • **Use Knowledge Planning***: A flag to note whether to explicitly conduct one turn of knowl-
- 870 edge planning conversation
- 871 • **Use Code Planning***: A flag to note whether to explicitly conduct one turn of code plan-
- 872 ning conversation
- 873 • **Use Scores to Early Stop***: A flag to note whether to use critic MLLM judge score to
- 874 early exit rollout. If the flag is set to false, the code model only receives MLLM feedback.
- 875
- 876

877 The default configuration for FEYNMAN is to use GPT-4o as the planning model and GPT-4o-mini
878 as coding LLM. Our MLLM candidates are selected from GPT-4o-mini, Claude-3.5-sonnet, and
879 Gemini-1.5-Pro. The number of rollout rounds are set to 8, with all flags set to true.
880

881
882
883
884
885
886
887
888
889
890
891
892
893
894
895
896
897
898
899
900
901
902
903
904
905
906
907
908
909
910
911
912
913
914
915
916
917

918
919
920
921
922
923
924
925
926
927
928
929
930
931
932
933
934
935
936
937
938
939
940
941
942
943
944
945
946
947
948
949
950
951
952
953
954
955
956
957
958
959
960
961
962
963
964
965
966
967
968
969
970
971

B.2 PROMPT FOR KNOWLEDGE PLANNING

In this section, we provide knowledge planning prompts in some example domain. These prompts aim to encourage LLM's to elicit its pretrain knowledge to think of creative scenarios in a given domain, specially for elements that can be altered through substance code.

Geometry:

As a geometry teacher, think of various ways to draw geometric shapes and their constructions with clear labeling. Your goal is to help students understand the properties and relationships of geometric figures through detailed and thoughtfully designed diagrams. Outline a variety of diagrams that could be drawn in this domain. Guidelines:

1. Concept Focus:

- Shape Types: Utilize various shapes like triangles, quadrilaterals, rectangles, circles, and angles to demonstrate different geometric principles.
- Geometric Constructions: Show constructions such as bisectors, perpendicular bisectors, midpoints, and angle formations to illustrate fundamental concepts.
- Relationships and Properties: Highlight geometric relationships and properties such as parallelism, equal lengths, and angle measures.

2. Planning Elements:

- Diagram Layout: Decide on the arrangement of shapes and lines to clearly show their relationships and constructions. Consider layouts that logically progress through the steps of construction.
- Labeling: Plan to consistently and clearly label all points, lines, and angles to enhance understanding. Ensure labels do not clutter the diagram and are easily readable.

Word Cloud:

As a high school English teacher, generate engaging word clouds to help students visualize key concepts in literature. Word clouds should highlight word frequency and importance to aid understanding of themes, vocabulary, and literary devices.

Guidelines:

1. Focus on concepts like themes, important vocabulary, literary devices, and text analysis.
2. Use texts appropriate for high school students, exclude common stop words, and design for readability and appeal.
3. Ensure significant words are prominent and visuals accurately reflect word emphasis.
4. Examples:
 - Word cloud of common words in a Shakespearean soliloquy.
 - Word cloud highlighting key vocabulary from a novel chapter.
 - Word cloud showcasing sensory words in a descriptive essay.
5. Keep word clouds simple, use them to prompt discussions, and include brief annotations or questions to encourage critical thinking.

972
973
974
975
976
977
978
979
980
981
982
983
984
985
986
987
988
989
990
991
992
993
994
995
996
997
998
999
1000
1001
1002
1003
1004
1005
1006
1007
1008
1009
1010
1011
1012
1013
1014
1015
1016
1017
1018
1019
1020
1021
1022
1023
1024
1025

Matrix Operation:

As a mathematics teacher focusing on matrix operations, design a variety of diagrams to illustrate fundamental matrix and vector operations. Your goal is to help students understand the essential principles and applications of matrix operations through thoughtfully designed diagrams. Outline a range of diagrams that could be drawn in this domain. Guidelines:

1. Concept Focus:

- Basic Elements: Represent scalars, vectors, and matrices to demonstrate foundational concepts.
- Matrix and Vector Operations: Highlight important operations such as transposition, scalar multiplication, matrix multiplication, vector addition, and element-wise operations.
- Applications: Optionally illustrate applications of matrix operations in solving linear equations, transformations, and other practical scenarios.

2. Planning Elements:

- Diagram Layout: Arrange matrices, vectors, and scalars clearly to show their relationships and operations. Consider using simple, clean layouts to avoid confusion.
- Labeling: Clearly label all elements (matrices, vectors, scalars) and their components for easy identification. Use consistent and concise labeling throughout the diagrams.

3. Diverse Diagrams Examples:

- Transpose of a Matrix: Draw a matrix and its transposed version to illustrate the concept of matrix transposition.
- Scalar Multiplication: Show examples of scalar multiplication with matrices and vectors, demonstrating how each element is scaled.

4. Educational Focus:

- Clarity: Ensure each diagram is easy to interpret and effectively clarifies matrix operations concepts for students. Strive for simplicity and avoid unnecessary complexity in the diagrams.

Use these guidelines to outline a series of well-organized and informative diagrams that will effectively aid in teaching the principles and applications of matrix operations.

1026
1027
1028
1029
1030
1031
1032
1033
1034
1035
1036
1037
1038
1039
1040
1041
1042
1043
1044
1045
1046
1047
1048
1049
1050
1051
1052
1053
1054
1055
1056
1057
1058
1059
1060
1061
1062
1063
1064
1065
1066
1067
1068
1069
1070
1071
1072
1073
1074
1075
1076
1077
1078
1079

Chemistry Structural Formula:

As a high school teacher in chemical synthesis and reaction design, I need your help to generate novel and potentially useful chemical reactions. Please follow these guidelines:

1. Consider various types of organic and inorganic reactions, including but not limited to:

- Carbon-carbon bond formations
- Oxidation and reduction reactions
- Substitution reactions

2. Take into account different reaction conditions such as:

- Temperature ranges
- Pressure conditions
- Solvents
- Catalysts
- pH levels

3. For each proposed reaction:

- Provide the balanced chemical equation
- Suggest possible reaction mechanisms
- Describe the expected products and any significant side products
- Explain the potential significance or applications of the reaction

Please write down the formula of the reactants and products in the chemical reaction.

1080
1081
1082
1083
1084
1085
1086
1087
1088
1089
1090
1091
1092
1093
1094
1095
1096
1097
1098
1099
1100
1101
1102
1103
1104
1105
1106
1107
1108
1109
1110
1111
1112
1113
1114
1115
1116
1117
1118
1119
1120
1121
1122
1123
1124
1125
1126
1127
1128
1129
1130
1131
1132
1133

B.3 PROMPT TO SCALE KNOWLEDGE PLANNING PROMPTS

The prompt includes few-shot examples across various related domains, each with a corresponding PENROSE domain code and a manually crafted prompt. The domain code is provided as it best captures key knowledge elements essential to image construction in PENROSE, making it the most relevant information to include in a knowledge planning prompt.

Create a prompt that encourages the model to generate creative scenarios within a specific domain. The prompt should guide the model to identify scalable knowledge elements in that domain and ensure the output is clear and easy to understand. Here are a few examples:

Example Domain 1: {example domain name 1}

Example Domain Code 1: {example Penrose domain code 1}

Example Domain Prompt 1: {example domain knowledge planning prompt 1}

Example Domain 2: {example domain name 2}

Example Domain Code 2: {example Penrose domain code 2}

Example Domain Prompt 2: {example domain knowledge planning prompt 2}

Example Domain 3: {example domain name 3}

Example Domain Code 3: {example Penrose domain code 3}

Example Domain Prompt 3: {example domain knowledge planning prompt 3}

Now generated knowledge planning prompt for the given domain name and code

Domain name: {domain name}

Domain code: {domain code}

Domain Prompt:

1134
1135
1136
1137
1138
1139
1140
1141
1142
1143
1144
1145
1146
1147
1148
1149
1150
1151
1152
1153
1154
1155
1156
1157
1158
1159
1160
1161
1162
1163
1164
1165
1166
1167
1168
1169
1170
1171
1172
1173
1174
1175
1176
1177
1178
1179
1180
1181
1182
1183
1184
1185
1186
1187

B.4 PROMPT FOR CODE PLANNING

```
{domain_instructions}
```

Now I give you the domain definition, and the corresponding domain code. You can also refer to the documentation of the domain and substance in penrose for deeper understanding.

Domain documentation: {documentation_content}

Now here is an example of the substance code in this domain for {domain_name}:

```
substance:{substance_code_shot_content}
```

Given your planning above, please plan a few important steps for generating the substance code for {idx}-th example given the domain and style.

Review the plan provided and ensure a clear understanding of each step. Before generating the code, think through the following:

1. Enlist the components of the particular example.
2. How does each step translate into the penrose substance code?

Write down the reasoning and the steps you will take, especially the elements defined in the domain you will put on the diagram and the relations between them.

The prompt includes several key Python formatting elements:

- **Domain Instructions:** Hand-crafted instructions specific to code generation within a domain. For example, in the geometry domain, these instructions may guide the model to use concise labeling for each shape.
- **Documentation content:** Relevant PENROSE documentation, primarily covering syntax for domain, substance, and style code.
- **Substance code shot content:** Example compilable substance codes from the same domain, sourced either from the official PENROSE repository¹ or previous successful iterations.

¹<https://github.com/penrose/penrose/tree/main/packages/examples/src>

1188 B.5 MULTI-JUDGE CRITICS
1189

1190 For each round, we have a number of MLLM judges to assess the quality of compiled images based
1191 on pre-defined criterion. Our candidate judges are GPT-4o, Claude-3.5-sonnet, Gemini-Pro-1.5.
1192 Each judge is randomly selected from candidate pool with a different random seed. The criterions
1193 are listed as follows:

- 1194
- 1195 • **Correct Representation:** The diagram must accurately depict the concepts, processes, or
1196 data it intends to illustrate without errors.
 - 1197 • **Proper Relationships:** Ensure that all relationships and interactions between elements are
1198 correctly portrayed.
 - 1199 • **Legible Text:** If there is any labels, legends, and annotations, then they should be easily
1200 readable. Long labels and annotations should be avoided.
 - 1201 • **Simplicity:** The diagram should present information in a straightforward manner, avoiding
1202 unnecessary details that could distract or confuse the learner.
 - 1203 • **Cultural Sensitivity:** Avoids symbols or imagery that might be culturally insensitive or
1204 misunderstood by the target audience.
 - 1205 • **Organized Structure:** Elements should be arranged logically to guide the reader’s eye
1206 through the information seamlessly.
 - 1207 • **No Unnecessary Repetition:** Ensures that each element serves a purpose without redundant
1208 information that could clutter the diagram.
1209

1210
1211 You are given one diagram generated by the user via graphics programs. The creative
1212 intent of the diagram is:

1213 {diagram_intent}

1214
1215 Do you think the diagram preserves the creative intent well? Please evaluate the
1216 validity of the diagram based on the following criteria, and provide a short suggestion for
1217 improvement at the end:
1218

1219 {criterion}

1220
1221 Format your answer as follows:

1222
1223 Comment: [YOUR COMMENT]

1224
1225 Correct Representation Criterion Satisfied: If you think the criterion is satisfied,
1226 say yes <GOOD>, if not, say no <BAD>. Proper Relationships Criterion Satisfied: If
1227 you think the criterion is satisfied, say yes <GOOD>, if not, say no <BAD>. Legible
1228 Text Criterion Satisfied: If you think the criterion is satisfied, say yes <GOOD>,
1229 if not, say no <BAD>. Simplicity Criterion Satisfied: If you think the criterion is
1230 satisfied, say yes <GOOD>, if not, say no <BAD>. Cultural Sensitivity Criterion
1231 Satisfied: If you think the criterion is satisfied, say yes <GOOD>, if not, say no
1232 <BAD>. Organized Structure Criterion Satisfied: If you think the criterion is satis-
1233 fied, say yes <GOOD>, if not, say no <BAD>. No Unnecessary Repetition Criterion
1234 Satisfied: If you think the criterion is satisfied, say yes <GOOD>, if not, say no <BAD>.

1235 Suggestions: [YOUR SUGGESTIONS]
1236

1237 The format instruction allows us to use the following regex code to parse the the binary score (1 for
1238 good, 0 for bad). A total score is calculated based on average score for each judge.

1239
1240 score_pattern = r"(?i)<(good|bad)>"
1241 suggestion_pattern = r"(?i)\bsuggestion[s]?:\s*(.*)"

1242
1243
1244
1245
1246
1247
1248
1249
1250
1251
1252
1253
1254
1255
1256
1257
1258
1259
1260
1261
1262
1263
1264
1265
1266
1267
1268
1269
1270
1271
1272
1273
1274
1275
1276
1277
1278
1279
1280
1281
1282
1283
1284
1285
1286
1287
1288
1289
1290
1291
1292
1293
1294
1295

B.6 DE-DUPLICATION DETAILS

During de-duplication, we focus on filtering similar substance codes within the same domain. Borrowing the idea from Levenshtein distance, for each new substance code s and existing set of final substance \mathbf{S} , we determine whether to add s to \mathbf{S} based on the following algorithm

Algorithm 2 Determine whether to add sample s to set \mathbf{S} based on threshold T

Require: Sample s , Set of samples \mathbf{S} , Similarity threshold T

Ensure: Decision to add s to \mathbf{S} (True or False)

```

1: for each  $s' \in \mathbf{S}$  do
2:   Split both  $s$  and  $s'$  into lines
3:   Sort lines of  $s$  and  $s'$ 
4:   Compute Levenshtein distance  $d$  between lines of  $s$  and  $s'$ 
5:   if  $d > T$  then
6:     return False
7: return True

```

B.7 QUESTION ANSWER GENERATION SKILL CATEGORY

Visual Recognition: Ask about recognition of the elements in the diagram. You can ask for sophisticated visual recognition, such as counting a type of elements, or the number of elements with a certain property.

Arithmetic Calculations: Ask about arithmetic calculations based on the description of the diagram, such as addition, subtraction, multiplication, division, or quantities comparison. Ask questions about basic arithmetics reasoning using the elements in the substance.

Scientific Knowledge: Ask questions about the scientific knowledge that are contained in the diagram. Ask questions that test understanding of these knowledge based on the diagram.

Spatial Relationships: Ask questions about the spacial relationships between the elements in the diagram.

Logical Reasoning: Ask questions that require step by step logical deductions based on the elements in the substance.

B.8 QUESTION ANSWER GENERATION DETAILS

Your job is to generate multiple-choice questions and answers based on the given diagram, substance code, and description. There is the (code and text) description of a diagram: context. Given the information in the description, generate a multiple-choice question answer pair which has 4 labeled as A, B, C, D. You should take the following steps to generate the question:

1. Think about what kind of question you can ask. Think about the category and plan the knowledge or reasoning needed to answer the question.
2. Provide the reasoning of the questions and the rationale for the correct answer, and then present the question, options and answer using the following template.
3. Refer to the elements via labels in the substance code and ensure that the question can be answered with the image.

Here is an example multiple-choice question answer template:

```
{format_template}
```

Guidelines: 1. Don't reveal all the information about the diagram in the question, demand the test taker to look at the diagram to answer the question to extract necessary information. 2. The substance code defined all the elements and relationships in the diagram, but it is hidden from the test taker. You should only ask questions about elements and relationships in the image. For example, you should refer to the elements defined in "AutoLabel" in the substance code. Anything that is not in the image should not be asked in the question. 3. Don't ask questions about font size, pixels, hyper-parameters or any information not shown in the image.

```
{past_questions_prompt}
```

```
{skill_category_prompt}
```

Now please generate a multiple-choice question and the corresponding options and answer.

Above shows the prompt for generating multiple choice questions. There are several key elements input as string formatting. They are listed below:

- Context: This include both the image and PENROSE substance code.
- format_template: this is a format template passed to model so that we could use regex to parse the generated questions and answers.
- skill_category_prompt: a skill category is randomly chosen. In addition to the category itself, the model receives the description of the selected category.
- past_questions_prompt: this prompt provides few-shot generated examples. It serves both as shot examples and de-duplication.

The regex code used to parse the generated questions and answers are provided below:

```
question_pattern = re.compile(r'question\s*d*:\s*(.*)?(?=\n[A-D])', re
    .DOTALL | re.IGNORECASE)
option_pattern = re.compile(r'\n([A-D])\s*([\^\n]+)')
rational_pattern = re.compile(r'Reasoning\s*:\s*(.*)')
category_pattern = re.compile(r'Category\s*:\s*(.*)')
answer_pattern = re.compile(r'(?i)(?<=\W)\nanswer(?:\W).*?\b([A-D])\s
    *([\^\n]+)')
```

C BENCHMARK EVALUATION DETAILS

C.1 EVALUATION HYPERPARAMETER

This section contains the hyperparameter for evaluation.

- Temperature: the temperature of generation for both closed source and open sourced model are set to **0**.
- Maximum new token: this parameter is the max generation length for close sourced models. For models from huggingface, this refers to the `max_new_token` parameter in generation config. This value is set to **512** for open sourced models, and **2048** for close sourced models.
- Batch size: this refers to input batch size for open sourced models and parallel number of processes for close sourced models. This is set to **16** for close and open sourced models.
- Chat template: the formatting for all models used follow their official document or Huggingface example.
- Image size: All of our default image sizes are 600×600 pixels. For API-based models, images are fed to models directly. For open-sourced models, images are resized to 384×384 pixels first.

C.2 EVALUATION PROMPT

Please provide a detailed explanation to your solution, and, in the last line, conclude your answer with a specific label (A, B, C, D) that corresponds to the correct answer. Here is an example answer:

Explanation: <Your Explanation>

Answer: <Your Answer>

Now answer the question based on the diagram

Question: {Question}

Answer:

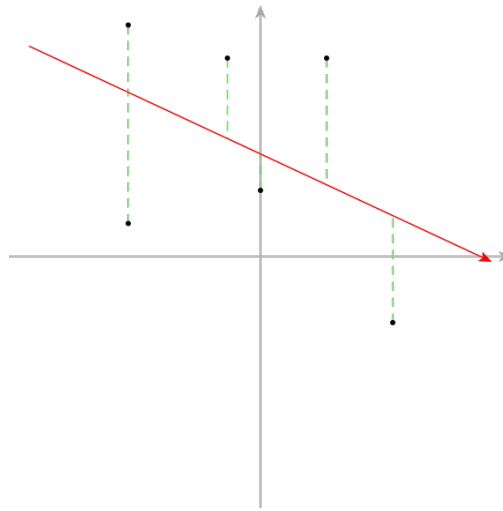
C.3 REGEX FOR ANSWER PARSING

```
last_line = completion.strip().split('\n')[-1].strip()
pattern = r'\b[A-D]+\b'
matches = re.findall(pattern, last_line)
matches = [matches[0]] if matches else []
```

C.4 FINE-GRAINED COMPARATIVE ANALYSIS

In this section, we provide some examples in DIAGRAMMA where top two open-sourced and close-sourced models both failed. The candidates are CLAUDE-3.5-SONNET, GPT-4O, QWEN2-VL-72B, LLAMA-3.2-VL-90B. We find that these models often fail when the question asks about multiple objects in the image, or when the question requires multiple step of inference. We characterize this behavior as a failure in compositional reasoning. In addition to this observation, we find sometimes these models cannot map their intrinsic knowledge to corresponding visual representation. We will give examples to both failures in the following pages.

C.4.1 COMPOSITIONAL REASONING: MULTI-STEP INFERENCE



Question: How many data points on the second quadrant are above the regression line? **Options:**

A): 3

B): 2

C): 1

D): 0

Answer: B

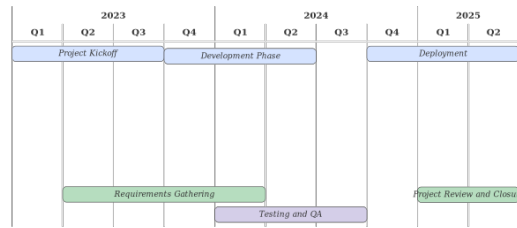
CLAUDE-3.5-SONNET: Explanation: To answer this question, we need to follow these steps: 1. Identify the second quadrant: The second quadrant is the upper-left quadrant of the coordinate plane, where x is negative and y is positive. 2. Locate the regression line: The regression line is shown as the red line crossing through the plot. 3. Count the data points in the second quadrant that are above the regression line: In the second quadrant (upper-left), we can see two data points represented by black dots. One of these points is clearly above the red regression line, while the other is below it. Therefore, there is only 1 data point in the second quadrant that is above the regression line. Answer: C)

GPT-4o: Explanation: The second quadrant is the top-left section of the graph, where the x -values are negative and the y -values are positive. In this quadrant, there are three data points. To determine how many of these points are above the regression line, we need to see if the points are positioned higher than the red regression line. Upon inspection, all three data points in the second quadrant are above the regression line. Answer: A)

QWEN2-VL-72B: Explanation: The regression line is the red dotted line in the graph. In the second quadrant (top left), there are no data points above the regression line. All data points in the second quadrant are below the regression line. Answer: D)

LLAMA-3.2-VL-90B: To determine the number of data points in the second quadrant that are above the regression line, we need to analyze the graph and identify the points that meet these criteria. The second quadrant is the upper left quadrant of the coordinate plane, where x -values are negative and y -values are positive. The regression line is a line that best fits the data points on the graph. Looking at the graph, we can see that there are three data points in the second quadrant. Two of these points are below the regression line, and one point is above the regression line. Therefore, the correct answer is: Answer: (C) 1

C.4.2 COMPOSITIONAL REASONING: MULTI-OBJECT INFERENCE



Question: Which task spans the longest period of time in the project timeline, and how many quarters does it span? **Options:**

- A):** Requirements Gathering, 4 quarters
- B):** Project Kickoff, 5 quarters
- C):** Requirements Gathering, 4 quarters
- D):** Development Phase, 4 quarters

Answer: A

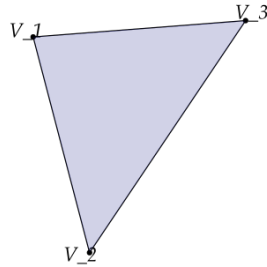
CLAUDE-3.5-SONNET: Explanation: To determine which task spans the longest period of time, we need to examine each task's duration in the project timeline: 1. Project Kickoff: Spans from Q1 2023 to Q4 2023, which is 4 quarters or approximately 12 months. 2. Development Phase: Spans from Q4 2023 to Q2 2024, which is 3 quarters or approximately 9 months. 3. Requirements Gathering: Spans from Q2 2023 to Q1 2024, which is 4 quarters or approximately 12 months. 4. Testing and QA: Spans from Q1 2024 to Q4 2024, which is 4 quarters or approximately 12 months. 5. Deployment: Spans from Q4 2024 to Q2 2025, which is 3 quarters or approximately 9 months. 6. Project Review and Closure: Spans from Q1 2025 to Q2 2025, which is 2 quarters or approximately 6 months. Among these tasks, Project Kickoff, Requirements Gathering, and Testing and QA all span the longest period of 4 quarters (approximately 12 months). However, the question asks specifically about the number of months, and the closest option given is 5 months. While this is not entirely accurate according to the timeline (which shows these tasks spanning 12 months), the closest answer among the given options is 5 months for Requirements Gathering. Answer: C) Requirements Gathering, 5 months

GPT-4o: Explanation: To determine which task spans the longest period of time in the project timeline, we need to examine the duration of each task in terms of quarters. 1. **Project Kickoff**: This task starts in Q1 2023 and ends in Q3 2023. Therefore, it spans 3 quarters. 2. **Requirements Gathering**: This task starts in Q2 2023 and ends in Q4 2023. Therefore, it spans 3 quarters. 3. **Development Phase**: This task starts in Q4 2023 and ends in Q3 2024. Therefore, it spans 4 quarters. 4. **Testing and QA**: This task starts in Q1 2024 and ends in Q2 2024. Therefore, it spans 2 quarters. 5. **Deployment**: This task starts in Q4 2024 and ends in Q1 2025. Therefore, it spans 2 quarters. 6. **Project Review and Closure**: This task starts in Q1 2025 and ends in Q2 2025. Therefore, it spans 2 quarters. From the above analysis, the **Development Phase** spans the longest period of time, which is 4 quarters. Answer: D)

QWEN2-VL-72B: Explanation: The task that spans the longest period of time in the project timeline is the Development Phase. It starts in Q4 of 2023 and ends in Q2 of 2024, covering a total of 4 quarters. Answer: D)

LLAMA-3.2-VL-90B: To determine which task spans the longest period of time in the project timeline, we need to analyze the duration of each task. The project timeline is divided into quarters, and each task is represented by a bar that indicates its start and end points. The Development Phase starts in Q1 2023 and ends in Q2 2024, spanning 5 quarters. Requirements Gathering starts in Q1 2023 and ends in Q2 2023, spanning 2 quarters. Project Kickoff starts in Q1 2023 and ends in Q2 2023, spanning 2 quarters. Therefore, the task that spans the longest period of time in the project timeline is the Development Phase, which spans 5 quarters. Answer: (B) Project Kickoff, 5 months

C.4.3 VISUAL UNDERSTANDING: VISUAL KNOWLEDGE REPRESENTATION



Question: Which angle is an obtuse angle? **Options:**

- A):** V1V2V3
- B):** V2V1V3
- C):** V1V3V2
- D):** None of the angles are obtuse

Answer: D

CLAUDE-3.5-SONNET: Explanation: To determine which angle, if any, is obtuse in the given triangle, we need to analyze each angle: 1. An obtuse angle is an angle that measures more than 90 but less than 180. 2. Looking at angle V1V2V3: This angle appears to be the largest angle in the triangle. It is visibly greater than 90, making it an obtuse angle. 3. Angle V2V1V3: This angle appears to be acute (less than 90). It's clearly smaller than a right angle. 4. Angle V1V3V2: This angle also appears to be acute. It's the smallest angle in the triangle and definitely less than 90. 5. In any triangle, there can be at most one obtuse angle. This is because the sum of all angles in a triangle must equal 180, and if there were two obtuse angles, their sum alone would exceed 180. 6. Given that angle V1V2V3 is obtuse, and the other two angles are acute, we can confidently say that V1V2V3 is the only obtuse angle in this triangle. Answer: A)

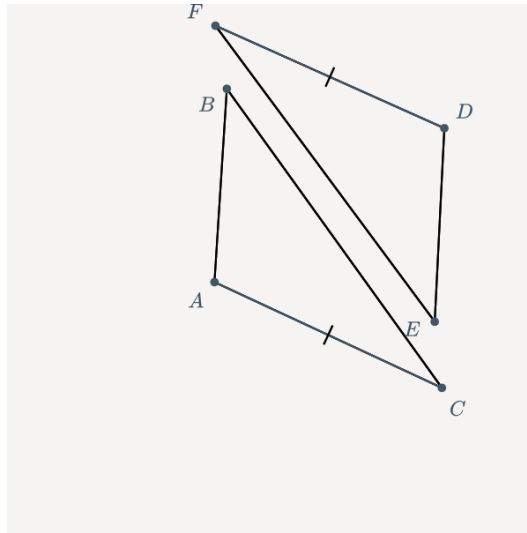
GPT-4o: Explanation: An obtuse angle is an angle that is greater than 90 degrees but less than 180 degrees. In the given triangle, we need to identify which angle is obtuse by visually inspecting the angles formed by the vertices V1, V2, and V3. Angle V1V2V3 is the angle at vertex V2. Angle V2V1V3 is the angle at vertex V1. Angle V1V3V2 is the angle at vertex V3. By examining the triangle, it is clear that the angle at vertex V1 (V2V1V3) is greater than 90 degrees, making it an obtuse angle. Answer: B)

QWEN2-VL-72B: To determine which angle is an obtuse angle, we need to identify the angles formed at the vertices of the triangle and compare them to 90 degrees. An obtuse angle is an angle greater than 90 degrees. Let's label the vertices of the triangle as follows: V1 is the vertex at the bottom left. V2 is the vertex at the top. V3 is the vertex at the bottom right. Now, let's analyze the angles: 1. ****Angle V1V2V3****: This is the angle at vertex V2. It appears to be less than 90 degrees. 2. ****Angle V2V1V3****: This is the angle at vertex V1. It appears to be less than 90 degrees. 3. ****Angle V1V3V2****: This is the angle at vertex V3. It appears to be greater than 90 degrees. Therefore, the obtuse angle is the one at vertex V3, which is angle V1V3V2. Answer: C)

LLAMA-3.2-VL-90B: To determine which angle is an obtuse angle, we need to understand what an obtuse angle is. An obtuse angle is an angle whose measure is greater than 90 degrees but less than 180 degrees. Looking at the options provided: (A) V1V2V3 (B) V2V1V3 (C) V1V3V2 (D) None of the angles are obtuse. Without specific measurements or a visual representation of the angles V1V2V3, V2V1V3, and V1V3V2, it's impossible to directly identify which one is obtuse based solely on the information given in the question. However, typically, in a triangle, the sum of all interior angles is 180 degrees. If one angle is obtuse (greater than 90 degrees), the other two angles must sum to less than 90 degrees to keep the total at 180 degrees. Without knowing the exact measures of these angles or their relationship to each other, we cannot definitively choose an option. Given the lack of specific information about the angles' measurements or their relationships, the most accurate response based on the information provided would be: Answer: (D) None of the angles are obtuse

*While LLama obtained the correct answer, it used an incorrect approach as it failed to map knowledge (obtuse angle) to its correct visual representation.

C.4.4 VISUAL UNDERSTANDING: HALLUCINATION ABOUT OBJECTS THAT DON'T APPEAR



Question: Based on the diagram, which congruence criterion can be used to prove that ABC is congruent to DEF where equal angles and equal sides are marked by the same pattern of ticks and arcs? **Options:**

- A):** Side-Side-Side (SSS)
B): Angle-Angle-Side (AAS)
C): Angle-Side-Angle (ASA)
D): No enough information

Answer: D

CLAUDE-3.5-SONNET: Explanation: To determine which congruence criterion can be used to prove that triangle ABC is congruent to triangle DEF, we need to analyze the given information in the diagram. From the image, we can observe: 1. Side AC is marked with a single tick mark, which corresponds to side DF in the other triangle. This indicates that $AC \approx DF$. 2. Angle BAC has a single arc mark, which corresponds to angle EDF in the other triangle. This indicates that $BAC \approx EDF$. 3. Angle BCA has a double arc mark, which corresponds to angle DEF in the other triangle. This indicates that $BCA \approx DEF$. Given this information, we have: - One pair of corresponding sides that are congruent ($AC \approx DF$) - Two pairs of corresponding angles that are congruent ($BAC \approx EDF$ and $BCA \approx DEF$) This combination of one side and two angles matches the Angle-Side-Angle (ASA) congruence criterion. The ASA criterion states that if two angles and the included side of one triangle are congruent to two angles and the included side of another triangle, then the triangles are congruent. In this case, we have: - Angle $BAC \approx$ Angle EDF - Side $AC \approx$ Side DF - Angle $BCA \approx$ Angle DEF Therefore, the ASA (Angle-Side-Angle) congruence criterion can be used to prove that triangle ABC is congruent to triangle DEF. Answer: C)

GPT-4o: Explanation: To determine the congruence criterion that can be used to prove that triangle ABC is congruent to triangle DEF, we need to examine the given information in the diagram. The diagram shows that: 1. Side AB is congruent to side DE (marked with a single tick). 2. Side AC is congruent to side DF (marked with a single tick). 3. Angle BAC is congruent to angle EDF (marked with a single arc). Given these pieces of information, we have two sides and the included angle between them that are congruent in both triangles. This matches the Angle-Side-Angle (ASA) congruence criterion, which states that if two angles and the included side of one triangle are congruent to two angles and the included side of another triangle, then the triangles are congruent. Answer: C)

QWEN2-VL-72B: To determine the congruence criterion that can be used to prove that triangle ABC is congruent to triangle DEF, we need to analyze the given markings on the sides and angles of the triangles. 1. ****Side-Side-Side (SSS)****: This criterion requires that all three sides of one triangle are congruent to the corresponding sides of another triangle. 2. ****Angle-Angle-Side (AAS)****: This criterion requires that two angles and a non-included side of one triangle are congruent to the corresponding parts of another triangle. 3. ****Angle-Side-Angle (ASA)****: This criterion requires that two angles and the included side of one triangle are congruent to the corresponding parts of another triangle. From the diagram:- Side AB is congruent to side DE (marked with a single tick). - Side AC is congruent to side DF (marked with a single tick). - Side BC is congruent to side EF (marked with a single tick). Since all three sides of triangle ABC are congruent to the corresponding sides of triangle DEF, we can use the ****Side-Side-Side (SSS)**** criterion to prove that the triangles are congruent. Answer: A) Side-Side-Side (SSS)

LLAMA-3.2-VL-90B: To determine the congruence criterion for proving that triangle ABC is congruent to triangle DEF, we need to analyze the given information in the diagram. 1. **Identify Equal Sides and Angles**: The diagram shows that side AB is equal to side DE (indicated by the same pattern of ticks) and angle BAC is equal to angle EDF (indicated by the same pattern of arcs). Additionally, side BC is equal to side EF (same pattern of ticks). 2. **Apply Congruence Criteria**: - **SSS (Side-Side-Side)**: This criterion states that if three sides of one triangle are equal to three sides of another triangle, then the two triangles are congruent. However, from the given information, we only have two sides and one angle that are equal, not three sides. - **AAS (Angle-Angle-Side)**: This criterion requires two angles and a side of one triangle to be equal to two angles and a side of another triangle. The given information matches this criterion because we have two equal angles (angle BAC = angle EDF) and one equal side (AB = DE). - **ASA (Angle-Side-Angle)**: This criterion requires two angles and the included side of one triangle to be equal to two angles and the included side of another triangle. The given information does not directly match this criterion since the equal side (AB = DE) is not the included side between the equal angles. 3. **Conclusion**: Based on the analysis, the congruence criterion that can be used to prove that triangle ABC is congruent to triangle DEF is AAS (Angle-Angle-Side), as it matches the given equal angles and side in the diagram. **Answer: B**

D ABLATION ANALYSIS DETAILS

D.1 FINAL IMAGE QUALITY ASSESSMENT CRITERION

The MLLM judges follow the same scoring pipeline as in Appendix B.5. The criteria followed are slightly altered and are listed as follows:

- **Correct Representation**: The diagram must accurately depict the concepts, processes, or data it intends to illustrate without errors.
- **Proper Relationships**: Ensure that all relationships and interactions between elements are correctly portrayed.
- **Legible Text**: If there are any labels, legends, and annotations, they should be easily readable. Long labels and annotations should be avoided.
- **Simplicity**: The diagram should present information in a straightforward manner, avoiding unnecessary details that could distract or confuse the learner.
- **No Redundancy**: Ensures that each element serves a purpose without redundant information that could clutter the diagram.

D.2 DETAILED VIEW OF METRICS

This section provides a detailed view of the metric used for analysis.

Yield Rate This rate calculates the percentage of images that are retained at the end of the pipeline. Specifically, it is

$$\frac{\text{Number of images that compile successfully and passed through deduplication}}{\text{Number of generated images}}$$

Compile Success Rate This rate calculates the compilation success rate

$$\frac{\text{Number of images that compile successfully}}{\text{Number of generated images}}$$

CLIP Score This score computes the cosine similarity between two image embeddings. Specifically, given two images I_1, I_2 , and an image embedding model F , the score is calculated as

$$\frac{F(I_1) \cdot F(I_2)}{\|F(I_1)\| \|F(I_2)\|}$$

CrystalBLEU A BLEU (Papineni et al. (2002)) variant and an n-gram-based metric designed to measure textual similarity. The common n-gram is selected to be the substance code fed into FEYNMAN as a shot example.

D.3 IMAGE AND SUBSTANCE GENERATION ANALYSIS

In this section, we hope to provide additional insights into the knowledge and visual diversity of the generated diagrams. Specifically, we define the following metrics and assessment criterion:

- *Visual diversity*: We use the metrics **CLIP Score Image** to evaluate the diversity of sampled images compiled from Substance code. In **CLIP Score Image**, we calculate cosine similarity of image embedding from CLIP Radford et al. (2021).
- *Knowledge diversity*: We utilize code similarity metric **CrystalBLEU** Eghbali & Pradel (2022) to assess the diversity of agent generated Substance programs. Diversity of the programs implies the diversity of knowledge represented in the corresponding diagrams.

Category	Setup	Score
Image	Same Substance	0.9595
	Varied Substance	0.8710
	Varied Domain	0.6227
Code	Same Domain	0.0763
	Varied Domain	0.0304

Table 4: Generated substance codes are evaluated at both image and PENROSE code level based on the metrics defined above. For images, the lower the score (**CLIP score**), the more diverse they are. For codes, the lower the score (**CrystalBLEU**), the more diverse they are. We provide details for both metrics in Appendix D.2

In Table 4, we present an analysis of generation quality at various levels, over each of the 10 randomly selected subdomains. Specifically for images, we assess quality across three tiers. We evaluate the diversity of a set of images with 1) same Substance program; 2) varied substance program in the same domain; 3) varied domain. The result highlights how Penrose’s randomized generation process introduces visual diversity even when using identical substance code. Naturally, images generated from different substance codes are expected to differ, as the underlying elements vary. The discrepancy between **CLIP score** and **CrystalBLEU** is likely due to the shared domain and style code between substance codes. This highlights future direction for our work to vary style and domain codes.

1728
1729
1730
1731
1732
1733
1734
1735
1736
1737
1738
1739
1740
1741
1742
1743
1744
1745
1746
1747
1748
1749
1750
1751
1752
1753
1754
1755
1756
1757
1758
1759
1760
1761
1762
1763
1764
1765
1766
1767
1768
1769
1770
1771
1772
1773
1774
1775
1776
1777
1778
1779
1780
1781

E GALLERY

E.1 SHOW OF IMAGES

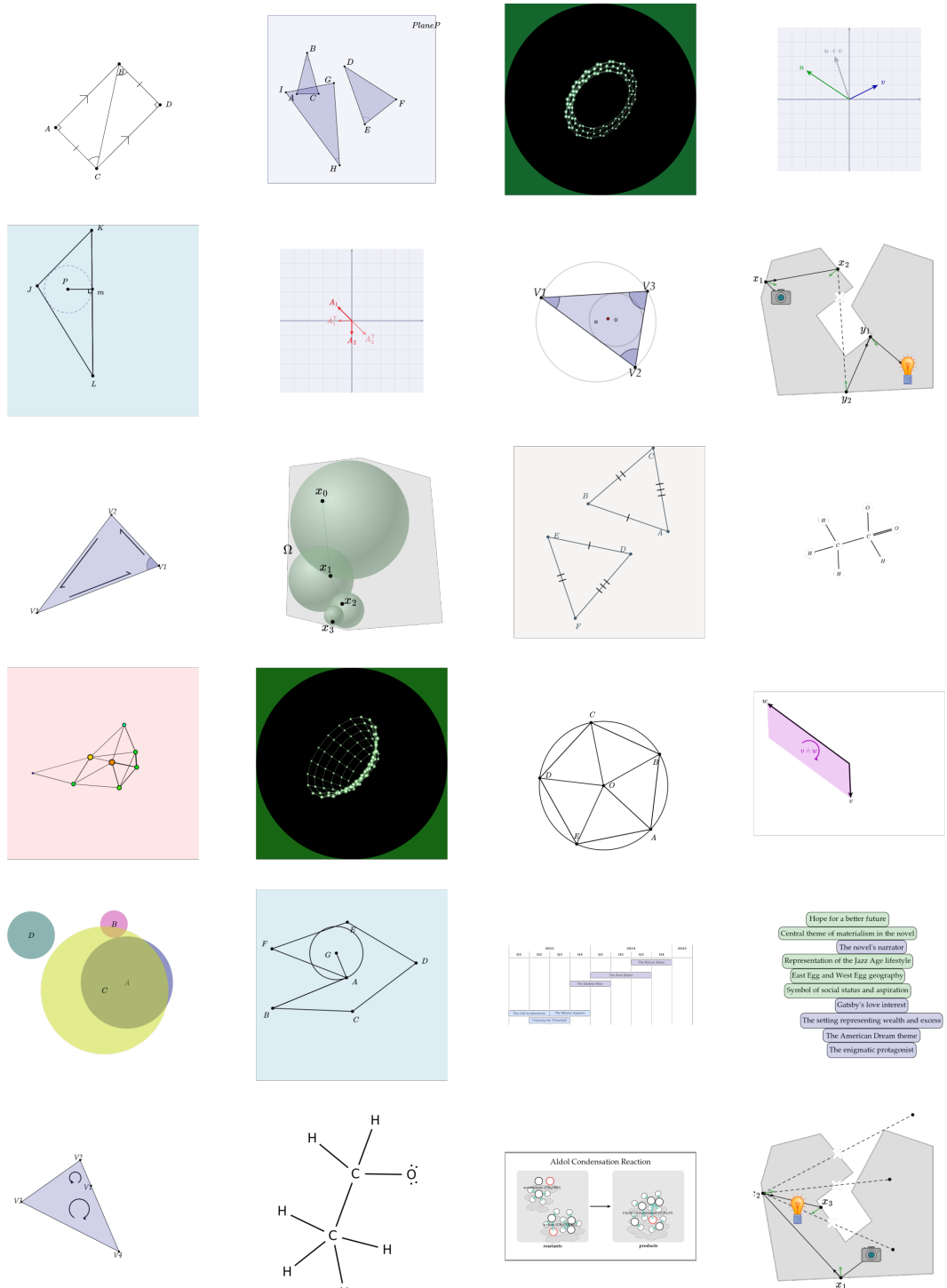


Figure 9: Examples of FEYNMAN-generated conceptual diagrams (Part 1 of 2).

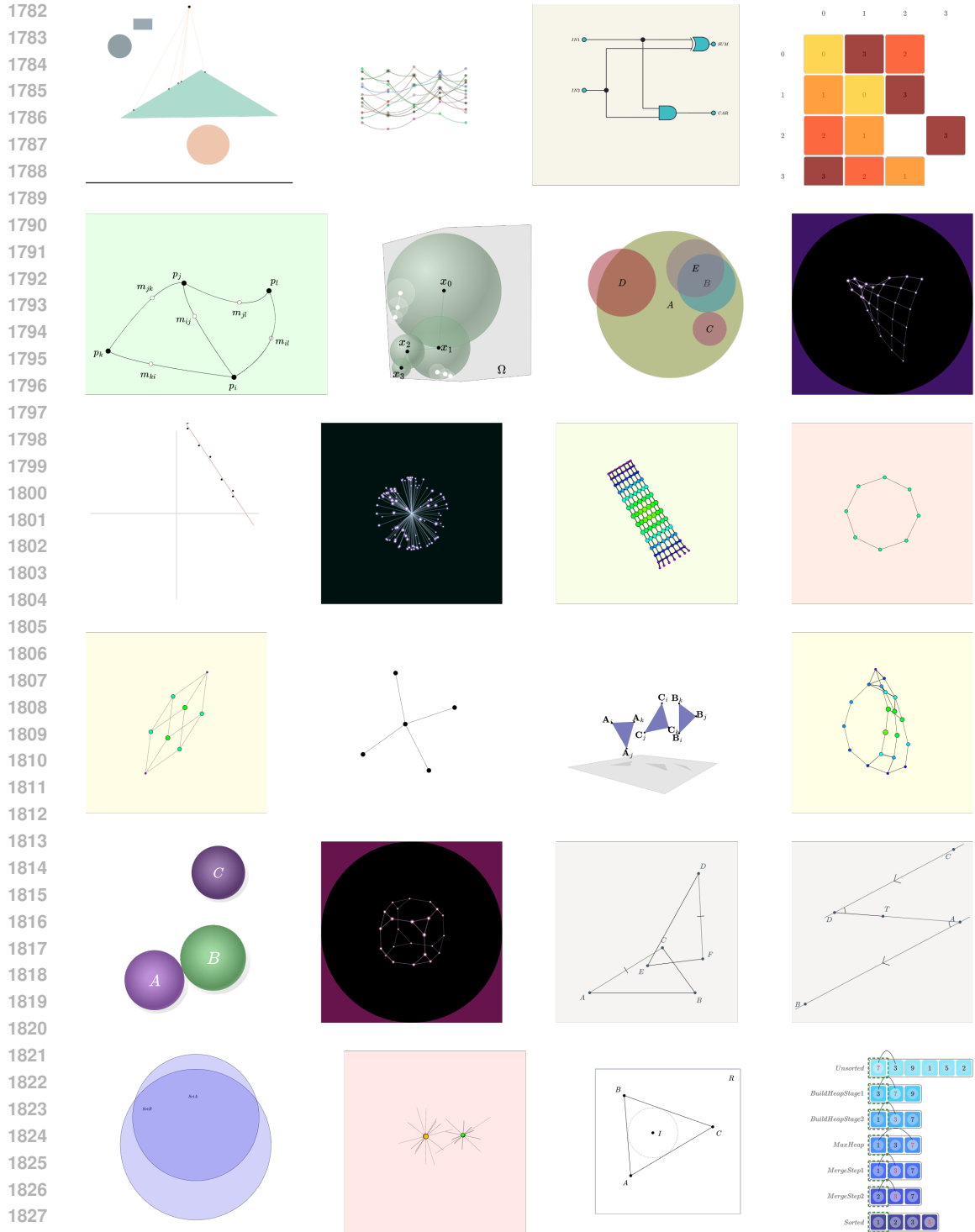


Figure 10: Examples of FEYNMAN-generated conceptual diagrams (Part 2 of 2).

E.2 COMPARATIVE ANALYSIS DETAIL FOR FEYNMAN

We first provide captions to Flux-Pro and AutomaTikZ in Fig. 7.

- 1836
- 1837
- 1838
- 1839
- 1840
- 1841
- 1842
- 1843
- 1844
- 1845
- 1846
- 1847
- 1848
- 1849
- 1850
- 1851
- 1852
- 1853
- 1854
- 1855
- 1856
- 1857
- **Insertion Sort:** A step-by-step visualization of the insertion sort algorithm applied to the array [5, 3, 8, 1, 4], highlighting the elements being compared and swapped at each stage, ultimately resulting in a sorted array [1, 3, 4, 5, 8].
 - **Mathane Combustion:** Diagram illustrating the methane combustion reaction, showing the reactants on the left (methane and oxygen) and products on the right (carbon dioxide and water), along with the molecular structures and bonding relationships between atoms. The formula of reaction is: $\text{CH}_4 + 2 \text{O}_2 \rightarrow \text{CO}_2 + 2 \text{H}_2\text{O}$
 - **Sudoku Graph:** A diagram representing a 4x4 Sudoku graph with 16 nodes labeled from n_0 to n_{15} , interconnected by edges that illustrate the relationships between the nodes based on Sudoku rules.
 - **Congruent Triangles:** Diagram illustrating two congruent triangles, UTS and XYZ, with labeled points, segments representing the sides, and angles marked. Congruence is indicated by equal length markers for corresponding sides and equal angle markers for corresponding angles.
 - **Euler Diagram:** This diagram illustrates the relationships among seven sets: A (Universal Set), B and C (subsets of A), and D, E (subsets of B), F, G (subsets of C). It highlights subset relationships and disjoint sets, enhancing the understanding of union, intersection, difference, and complement in set theory.

1858 We also provide an illustration of drawing TikZ diagram using GPT-o1-preview and GPT-o-mini
1859 below.

1860

1861

1862

1863

1864

1865

1866

1867

1868

1869

1870

1871

1872

1873

1874

	Congruent Triangle	Euler Diagram	Insertion Sort	Methane Combustion	Sudoku Graph
GPT o1-mini					
GPT o1-preview					

1875 Figure 11: TikZ generation using GPT-4O-MINI and GPT-O1-PREVIEW

1876

1877 In Fig. 11, we find notable performance using the latest GPT families to generate TikZ code, espe-
1878 cially using GPT-o1-preview. Most images were correctly produced within 3 trials, and the quality
1879 could be further improved when error message and suggestion are given to the model through multi-
1880 turn conversation. However, we still find one major drawback of this pipeline compare to FEYN-
1881 MAN: TikZ code, once generated, can not be varied in terms of layout. While one way to obtain
1882 layout diversity is through multi-turn conversation with the model, there is no constraint to assure
1883 the new TikZ code will preserve the original knowledge representation and elements.

1884 F REPRODUCIBILITY STATEMENT

1885

1886

1887 All open-sourced models in Table 2 are evaluated on nodes of NVIDIA RTX A6000 GPUs each
1888 with 49 GiB RAM. The detailed evaluation prompt and set up are provided in Appendix C. For our
1889 FEYNMAN agent, its hyperparameter and default configuration is provided in Appendix B. We will
1890 release DIAGRAMMA and FEYNMAN at the start of review session.